



UNIVERSITY OF LEEDS

This is a repository copy of *A Review Of Fault Sealing Behaviour And Its Evaluation In Siliciclastic Rocks*.

White Rose Research Online URL for this paper:
<http://eprints.whiterose.ac.uk/88994/>

Version: Accepted Version

Article:

Pei, Y, Paton, DA, Knipe, RJ et al. (1 more author) (2015) A Review Of Fault Sealing Behaviour And Its Evaluation In Siliciclastic Rocks. *Earth-Science Reviews*, 150. 121 - 138. ISSN 0012-8252

<https://doi.org/10.1016/j.earscirev.2015.07.011>

© 2015, Elsevier. Licensed under the Creative Commons Attribution-NonCommercial-NoDerivatives 4.0 International
<http://creativecommons.org/licenses/by-nc-nd/4.0/>

Reuse

Unless indicated otherwise, fulltext items are protected by copyright with all rights reserved. The copyright exception in section 29 of the Copyright, Designs and Patents Act 1988 allows the making of a single copy solely for the purpose of non-commercial research or private study within the limits of fair dealing. The publisher or other rights-holder may allow further reproduction and re-use of this version - refer to the White Rose Research Online record for this item. Where records identify the publisher as the copyright holder, users can verify any specific terms of use on the publisher's website.

Takedown

If you consider content in White Rose Research Online to be in breach of UK law, please notify us by emailing eprints@whiterose.ac.uk including the URL of the record and the reason for the withdrawal request.



eprints@whiterose.ac.uk
<https://eprints.whiterose.ac.uk/>

1 **A review of fault sealing behaviour and its evaluation in siliciclastic**
2 **rocks**

3 Yangwen PEI^{a, b, *}, Douglas A. PATON^b, Rob J. KNIFE^c, Kongyou Wu^a

4 a School of Geosciences, China University of Petroleum, Qingdao 266580, PR China

5 b School of Earth & Environment, University of Leeds, Leeds, LS2 9JT, England

6 c Rock Deformation Research, West Riding House, Leeds, LS1 5AA, England

7 * Corresponding author. Email: peiyangwen@163.com

8 **Abstract**

9 Faults can be either conduits or retarders for fluid flow. As the presence of
10 faults increases the risks for hydrocarbon exploration, the sealing behaviour
11 of a fault zone has been a focus for geological studies in the past 30 years.
12 Due to the widespread occurrence of fault zones, either in extensional or
13 contractual regimes, knowledge about the fault sealing behaviour is of
14 great importance to a wide spectrum of disciplines in geosciences, for
15 instance, structural geology, geochemistry, petroleum geology, etc.
16 Geologists have extensively study the sealing properties of a fault zone over
17 the last decades, ranging from fault zone architecture, fault seal types, fault
18 seal processes, fault rock classification, research methods and controlling
19 factors.

20 Although there have not been universal agreements reached on the fault
21 seal classifications, two types of fault seals have already been recognized,
22 which are juxtaposition seals and fault rock seals. The early foundation of
23 Allan map and triangle juxtaposition diagram allows the investigation on the

24 effects of stratigraphic juxtaposition between hanging wall and footwall on
25 the sealing properties of a fault zone. The study on the detailed fault zone
26 architecture also implies the importance of fault arrays that increase the
27 complexity of overall stratigraphic juxtaposition between hanging wall and
28 footwall. The fault seal processes and their generated fault rocks play an
29 important control on sealing properties of a fault zone. Temperature and
30 stress history, which are closely related to burial history, are also found to
31 control the sealing capacity of a fault zone to some extent. The methods
32 such as stratigraphic juxtaposition, clay smear indices, microstructural
33 analysis and petrophysical assessment has significantly boosted the
34 research of fault sealing behaviour. However, further research is still needed
35 to increase the effectiveness of present fault seal analysis.

36 **Keywords:** fault zone architecture, fault seal process, fault rocks,
37 hydrocarbon sealing behaviour

38 **1. Introduction**

39 In petroleum exploration and production, as faults can behave as i) conduits,
40 ii) barriers or iii) combined barrier-conduit structures for hydrocarbon
41 migration, the presence of faults increases the risks for hydrocarbon drilling,
42 exploration and development. In order to avoid or minimise the risks, the
43 way in which faults and fractures affect the hydrocarbon migration has
44 attracted the interest of geologists. Previous research (e.g., Allan, 1989;
45 Bouvier et al., 1989; Schowalter, 1979; Smith, 1966; Smith, 1980; Watts,
46 1987) has studied the fault behaviour and proposed many fundamental
47 principles that control the fault sealing properties within oil/gas reservoirs. In
48 the recent 20 years, the abundance of data, including seismic reflection data,

49 structural and micro-structural analysis from both core and field rock
50 samples, wellbore and production data of oil/gas fields, makes it possible to
51 conduct fault seal analysis to predict fault-sealing properties.

52 The progress in understanding the faulting processes (Balsamo et al., 2010;
53 Caine et al., 1996; Childs et al., 2009; Childs et al., 1996b; Walsh et al.,
54 2003), the fault rock development (Fisher and Knipe, 1998; Jolley et al.,
55 2007b; Knipe, 1989; Knipe et al., 1997; Tueckmantel et al., 2010), the fault
56 geometry (Jolley et al., 2007b; Peacock and Sanderson, 1991; Peacock and
57 Sanderson, 1992; Peacock and Sanderson, 1994; Walsh et al., 2003) and
58 the fault population (Billi et al., 2003; Cowie et al., 1996; Cowie and Scholz,
59 1992; Cowie et al., 1993; Faulkner et al., 2010; Kolyukhin et al., 2010; Walsh
60 et al., 2003) has provided a platform for improving the accuracy of fault
61 sealing analysis. The studies on the relationship between different fault
62 parameters, e.g., fault length, fault displacement and fault thickness, has
63 significantly promoted the understanding the effect of fault architecture on
64 fault compartmentalization (Faulkner et al., 2003; Fossen et al., 2007; Torabi
65 and Berg, 2011). Knipe et al. (1992a; 1992b; 1994), Fisher and Knipe (1998;
66 2001), Fisher et. al. (2003; 2009) and Jolley et. al. (2007a; 2007b) also
67 highlighted the importance of the fault zone complexity and the petrophysical
68 properties of the fault rocks in the evaluation of fault-sealing capacity. Firstly,
69 the fault zone development can involve strain being accommodated by a
70 complex array of faults not just a single, through-going fault; secondly, the
71 sealing capacity of the fault zones may vary significantly depending on the
72 composition of the host rocks that are entrained into the fault zones. Given
73 the important control of fault zone complexity and petrophysical properties of

74 the fault rocks, their controlling factors have been considered in recent
75 studies:

76 i) the changing chemical/physical processes with time, e.g., the
77 burial/temperature history (Fisher et al., 2003; Fossen et al., 2007; Jolley et al.,
78 2007b) and the amount/rate of strain (Balsamo et al., 2010; Faulkner et al.,
79 2010; Fossen and Bale, 2007);

80 ii) the diagenetic processes that affect the fault sealing capacity, e.g.,
81 disaggregation, clay/phyllsilicate smearing, cataclasis, pressure solution and
82 cementation (Faulkner et al., 2010; Fossen et al., 2011; Tueckmantel et al.,
83 2010).

84 Although geologists have also realized the importance of the fault zone
85 architecture within carbonates and its sealing properties in recent years
86 (Agosta et al., 2012; Brogi and Novellino, 2015; Collettini et al., 2014;
87 Faulkner et al., 2003; Fondriest et al., 2012; Korneva et al., 2014; Rotevatn
88 and Bastesen, 2014), majority of fault sealing analysis has still focused on
89 the fault zone architecture and fault seal analysis in siliciclastic reservoirs
90 since 1980s. Apparently, the studies of fault zone architecture and
91 hydrocarbon sealing behaviour in siliciclastic reservoirs are more thorough
92 and therefore this review paper has focused on siliciclastic reservoirs by
93 integrating the previous studies of different perspectives. In this paper, we
94 firstly review the sealing behaviour of a fault zone in the aspects of fault
95 zone architecture, fault seal types, fault seal processes, fault rock
96 classification, methods and controlling factors; and then discuss the
97 limitations of the current models/methods to give suggestions on the future
98 work on fault zone architecture and its effects on hydrocarbon sealing
99 behaviour.

100 **2. Fault Zone Architecture**

101 Understanding the effects of stress on given rock volumes is of importance
102 to the investigation of rock deformation mechanisms and their effects on
103 hydrocarbon sealing behaviour of a fault zone. The competent rocks (e.g.
104 sandstones or carbonates) are inclined to brittle deformation (e.g., faulting),
105 whereas the incompetent rocks (e.g., mudstones or shales) prefer to ductile
106 deformation (e.g., folding). In previous studies focusing on the deformation
107 mechanisms of the mechanically layered sequence, it has been reported
108 that the faults tend to form first in the brittle beds (e.g. cemented sandstones
109 or carbonates); while the weak/ductile beds (e.g. clay beds) deform by
110 distributed shear to accommodate the overall strain ([Childs et al., 1996a](#);
111 [Eisenstadt and De Paor, 1987](#); [McGrath and Davison, 1995](#); [Peacock and](#)
112 [Sanderson, 1992](#); [Schöpfer et al., 2006](#)). Several quantitative dynamic
113 models have been presented (e.g., [Egholm et al., 2008](#); [Welch et al., 2009a](#);
114 [Welch et al., 2009b](#); [Welch et al., 2015](#)) to analyse the mechanics of
115 clay/shale smearing along faults in layered sand and shale/clay sequences.
116 These models predict that the isolated initial faults formed within the brittle
117 beds will grow until eventually they link up with increasing strain, by
118 propagating across the ductile intervals to create a complex fault zone
119 architecture ([Childs et al., 1996a](#); [Peacock and Sanderson, 1991](#); [Walsh et](#)
120 [al., 2003](#); [Walsh et al., 1999](#); [Welch et al., 2009a](#); [Welch et al., 2009b](#)). Many
121 natural examples support those previous studies on detailed fault zone
122 architecture, e.g., the deformed interbedded sandstones and shales derived
123 from the Cutler Formation juxtaposed against limestone from the Honaker
124 Trail Formation near the entrance to Arches National Park ([Davatzes and](#)

125 [Aydin, 2005](#)); the outcrop studies from a minor normal-fault array exposed
126 within Gulf of Corinth rift sediments, Central Greece ([Loveless et al., 2011](#));
127 and the multilayer systems in the South-Eastern basin, France ([Roche et al.,](#)
128 [2012](#)). Fault zone models defining the fault zone architecture have also been
129 proposed, e.g., the fault zone model in crystalline rocks ([Caine et al., 1996](#));
130 the fault zone model in poorly lithified sediments ([Heynekamp et al., 1999](#);
131 [Rawling and Goodwin, 2003](#); [Rawling and Goodwin, 2006](#)); and the dynamic
132 fault zone models within poorly consolidated sediments by [Balsamo et. al.](#)
133 ([2010](#)) and [Loveless et al. \(2011\)](#).

134 As reviewed by [Knipe et. al. \(1997; 1998\)](#), fault zone geometry and fault
135 population play an important control on the fluid flow properties of fault
136 zones. The internal structures of individual fault zones need to be
137 considered because it affects the distribution of fault rocks and stratigraphic
138 juxtaposition (e.g., [Faulkner et al., 2010](#); [Rawling et al., 2001](#); [Walsh et al.,](#)
139 [1998](#); [Yielding et al., 1996](#)). For example, in the fault core and damage zone
140 model of [Caine et. al. \(1996\)](#), the fault core was taken as a barrier and the
141 damage zone was taken as a conduit for cross-fault fluid flow (Fig.1a);
142 however, [Faulkner et. al. \(2010; 2003\)](#) found that the intricate internal
143 structures of a fault zone can potentially lead to high degree of permeability
144 heterogeneity and anisotropy (Fig.1b). Many case studies have supported
145 these results, e.g., the fault zone structure and slip localization ([Choi et al.,](#)
146 [2015](#); [Collettini et al., 2014](#); [Fondriest et al., 2012](#)), the fluid flow properties
147 of a relay zones ([Fachri et al., 2013a](#); [Qu et al., 2015](#); [Rotevatn et al., 2007](#)),
148 etc.

149 Fig.1 Typical fault zone structures (Faulkner et al., 2010). (a) Shows a single
150 high-strain core surrounded by a fractured damage zone (Caine et al.,
151 1996) and (b) shows multiple cores model, where many strands of
152 high-strain material enclose fractured lenses (Faulkner et al., 2003).
153 The diagrams of fracture density and permeability indicate that the
154 complexity of fault zone geometry and fault population can play
155 important control on the fluid flow properties.

156 3. Fault seal types

157 Although there have not been universal agreements reached on the fault
158 seal classifications, two types of fault seals have already been recognized,
159 which are juxtaposition seals and fault rock seals (e.g., Cervený et al., 2004;
160 Faulkner et al., 2010; Jolley et al., 2007a; Jones and Hillis, 2003; Knipe,
161 1992a; Knipe et al., 1997; Knott, 1993).

162 3.1. Juxtaposition seals

163 Juxtaposition seals are associated with cases where cross fault juxtaposition
164 with low permeability non-reservoir units occurs and have been well
165 described in previous studies (Allan, 1989; Knipe, 1997). When a sequence
166 of beds is cut by faults, the hanging wall can be considered to move
167 downward for normal faults; upward for thrust faults; and laterally for strike
168 slip faults. The relative movement between the two walls of the faults gives
169 rise to the occurrence of juxtaposition between the rocks with different
170 lithology or petrophysical properties in the hanging wall and the footwall. As
171 rocks with different lithology usually have different petrophysical properties
172 (e.g. different porosity, permeability, capillary entry pressure), there will be a
173 permeability gradient between different rocks juxtaposed between the

174 hanging wall and the footwall. Juxtaposition seals between the hanging wall
175 and the footwall can be produced by this process. For instance, it is possible
176 to form juxtaposition seals when a sandstone bed is juxtaposed with a
177 mudstone/shale bed; in contrast, it may not form a juxtaposition seal when a
178 sandstone bed juxtaposes with a sandstone bed.

179 Fig.2 is a schematic diagram demonstrating the occurrence of the
180 juxtaposition seals. As the hanging wall moves downward relative to the
181 footwall, different stratigraphic units (A: mudstone; B: sandstone; C:
182 mudstone) from the hanging wall and the footwall juxtapose against each
183 other. For example, the mudstone bed (A) of the hanging wall juxtaposes
184 against the sandstone bed (B) of the footwall (polygon I); B of the hanging
185 wall juxtaposes against B of the footwall (polygon II); and B of the hanging
186 wall juxtaposes against C of the footwall (polygon III). As sandstone
187 presents higher permeability and lower capillary entry pressure than
188 mudstone, the juxtaposition seals can happen in polygon I and polygon III,
189 but do not happen in polygon II. Apart from the lithology of the hanging wall
190 and footwall, the layer thickness and fault throw are also of importance to
191 juxtaposition seals. For a permeable layer (e.g., sandstones) with a certain
192 thickness, the permeable layers can be self-juxtaposed to form conduits for
193 hydrocarbon migration if the fault throw was smaller than the thickness,
194 whereas juxtaposition seals may occur if the fault throw exceeded the
195 thickness. For a certain fault throw, a permeable layer thicker than the fault
196 throw can be self-juxtaposed to form conduits for hydrocarbon migration,
197 whereas a permeable layer thinner than the fault throw can possibly
198 generate juxtaposition seals.

199 Fig.2 A schematic diagram shows stratigraphic juxtaposition between the
200 hanging wall and footwall (modified from Knipe et al., 1997).
201 Juxtaposition seal can occur when low-permeable rocks in the hanging
202 wall juxtapose against high-permeable rocks in the footwall (e.g.,
203 polygon I and III).

204 **3.2. Fault rock seals**

205 According to terminology for structural discontinuities reviewed by Schultz
206 and Fossen (2008), the term 'fault' is defined as a single plane that has been
207 called a slip plane or shear fracture, whereas the term 'fault zone' is a
208 tabular region containing a set of parallel or anastomosing fault surfaces. As
209 shown in natural examples (e.g., Fig.1), many faults are not single-plane
210 faults but composed of a series of fault planes or networks of small fault
211 segments that form fault zones (Caine et al., 1996; Childs et al., 1996a;
212 Childs et al., 1996b; Faulkner et al., 2010; Knipe et al., 1997). Different fault
213 rocks are then generated when different types of host rocks are entrained
214 into the complex fault zones during faulting (Fisher and Knipe, 1998; Fossen
215 et al., 2007; Knipe et al., 1997; Knipe et al., 1998; Manzocchi et al., 2010;
216 Ottesen Ellevset et al., 1998). The study of Watts (1987) highlighted that
217 most faults/fault zones were membranes or flow retarders with different
218 properties of transmissibility or permeability. As the sealing properties of
219 fault rocks can be evaluated by the permeability and the capillary threshold
220 pressure (Fisher and Jolley, 2007; Fisher and Knipe, 2001; Watts, 1987), the
221 fluid flow across the fault zones will not happen unless the capillary
222 threshold pressure is reached. Therefore, the petrophysical properties of the

223 fault rocks, such as the capillary threshold pressure and permeability control
224 the hydrocarbon sealing properties of faults/fault zones.

225 As pointed out (Fisher and Knipe, 1998; Knipe et al., 1997), the composition
226 of the host sediments at the time of deformation determines the deformation
227 mechanisms, microstructures and petrophysical properties of the fault rocks
228 within the fault zones; and therefore fault rock seals may occur if fault rocks
229 with low permeability and high capillary threshold pressure are generated
230 within the fault zones.

231 **4. Fault Seal Processes**

232 The fundamental fault seal processes that give rise to the occurrence of fault
233 related permeability barriers have been studied in detail in the past 30 years
234 (e.g., Fisher et al., 2003; Fisher and Knipe, 1998; Fisher et al., 2009; Fossen
235 and Bale, 2007; Fossen et al., 2007; Fossen et al., 2011; Knipe, 1989; Knipe,
236 1992a; Knipe, 1993a; Knipe, 1993b; Knipe et al., 1998; Tueckmantel et al.,
237 2010). Five types of fault seal processes have been identified, which are: (i)
238 clay/phyllosilicate smearing; (ii) cementation; (iii) cataclasis; (iv) diffusive
239 mass transfer by pressure solution or quartz cementation; and (v) porosity
240 reduction by disaggregation or mixing. However, as Knipe (1997) pointed out,
241 these five fault seal processes can either perform individually during
242 deformation or combine interactively with each other.

243 **4.1. Clay/Phyllosilicate Smearing**

244 As continuous clay/phyllosilicate smear has very low porosity and
245 permeability (Smith, 1966; Smith, 1980), it acts as an extremely effective
246 fluid flow barrier and therefore many studies have focused on this fault seal
247 process. For example, deformation induced shearing of clays/phyllosilicates

248 has been discussed in previous studies (e.g., Aydin and Eyal, 2002; Bouvier
249 et al., 1989; Fulljames et al., 1997; Gibson, 1994; Yielding et al., 1997).

250 Three principle means of clay/phyllosilicate smearing are proposed by
251 Lindsay et al. (1993), which are:

- 252 a). abrasion of clay/phyllosilicate when it is moving past sandstones;
- 253 b). shearing and ductile deformation of beds (with high clay/phyllosilicate
254 content, e.g. shale or mudstone beds) between hanging wall and footwall;
- 255 c). injection of clay/phyllosilicate materials during fluidisation.

256 It is suggested that the continuity of clay/phyllosilicate smearing is
257 determined by a series of parameters including the sedimentary lithification
258 state, the effective stress, the confining pressure, the strain rate and the
259 mineralogy (Fisher and Knipe, 1998).

260 Several algorithms have been proposed to evaluate the fault sealing
261 properties quantitatively, either based on the continuity of clay/phyllosilicate
262 smears or average clay content within the fault zones, e.g., Clay Smear
263 Potential (CSP) (Bouvier et al., 1989; Fulljames et al., 1997), Shale Smear
264 Factor (SSF) (Lindsay et al., 1993), Shale Gouge Ratio (SGR) (Yielding et
265 al., 1997) and Scaled Shale Gouge Ratio (SSGR) (Ciftci et al., 2013). These
266 algorithms evaluate the fault sealing properties by considering the re-
267 distribution of mudstone/shale beds or the clay/phyllosilicate content of the
268 beds in sheared fractures. Empirically, the stacking sequences with high
269 clay/phyllosilicate content are likely to form fault zones with low permeability.
270 During the deformation of fault rocks, there can be two competing
271 compaction mechanisms which are the mechanical compaction and
272 chemical compaction (Fisher and Knipe, 2001). These two compaction

273 mechanisms affect fault rock properties depending on the clay/phyllsilicate
274 content of the host rocks. For example, faults developed in impure
275 sandstones (clay content of 15-25%) experienced enhanced chemical
276 compaction (e.g., grain-contact quartz dissolution), whereas faults in clay-
277 rich sandstones (clay content of >25%) are dominated by mechanical
278 compaction. The higher clay/phyllsilicate content in host rocks can
279 significantly decrease the effective quartz surface area, which lead to the
280 inhibition of the chemical compaction (e.g., quartz cementation) (Fisher and
281 Knipe, 1998). The competition between the two mechanisms results in the
282 relationship between clay/phyllsilicate content and fault sealing properties
283 (e.g., porosity, permeability, capillary pressure) being highly complicated and
284 can even lack correlation. Therefore, the algorithms, such as CSP (Bouvier
285 et al., 1989; Fulljames et al., 1997), SSF (Lindsay et al., 1993), SGR
286 (Yielding et al., 1997) and SSGR (Ciftci et al., 2013), should be used with
287 caution when evaluating the fluid flow properties of the fault zones.

288 **4.2. Cementation**

289 The most common result of deformation related cementation includes
290 cemented faults or fractures (Fisher and Knipe, 1998; Fisher and Knipe,
291 2001; Fisher et al., 2009; Fossen and Bale, 2007; Fossen et al., 2011;
292 Tueckmantel et al., 2010). The microstructures of these features provide
293 important evidence for studying the mechanisms and timing of the
294 cementation processes. As faults/fractures may perform as conduits for fluid
295 flow, the flow behaviour of faults/fractures is sensitive to quartz precipitation
296 because within the fault zones there are both quartz sources (from
297 dissolution) and nucleation sites for potential cementation. The source for

298 cementation can be internal or external, but [Fisher and Knipe \(1998\)](#) pointed
299 out that natural oil/gas field examples do not always require that an external
300 fluid source controls the sealing properties of the fault zones, especially at a
301 large scale where the external fluids may not promote continuous
302 cementation for extensive sealing.

303 As there may be impure sandstones containing clay minerals, it is important
304 to understand the effects of clay minerals on the quartz cementation, which
305 has been well established in previous studies (e.g., [Bjorkum, 1996](#); [Dewers
306 and Ortoleva, 1991](#); [Fisher and Knipe, 1998](#); [Fisher and Knipe, 2001](#);
307 [Fossen and Bale, 2007](#); [Fossen et al., 2011](#); [Heald, 1955](#); [Oelkers et al.,
308 1996](#)). It is suggested that small concentrations of clay/phyllosilicate
309 minerals in sandstones increase the potential of cementation as the
310 clay/phyllosilicate minerals can act as a local source for cementation
311 ([Dewers and Ortoleva, 1991](#); [Fisher et al., 2003](#); [Fisher et al., 2009](#); [Heald,
312 1955](#); [Knipe, 1993a](#); [Oelkers et al., 1996](#)). However, high clay/phyllosilicate
313 contents can lead to the clay/phyllosilicate-coating on the quartz grains,
314 which decreases the effective quartz grain surface area available for
315 cementation ([Cecil and Heald, 1971](#); [Fisher et al., 2003](#); [Fossen and Bale,
316 2007](#); [Fossen et al., 2011](#); [Tada and Siever, 1989](#); [Walderhaug, 1996](#)).

317 **4.3. Cataclasis**

318 Cataclasis involves grain fracturing and can reduce the porosity and the
319 permeability as well as increase the capillary threshold pressure of rocks
320 within fault zones (e.g., [Antonellini and Aydin, 1994](#); [Antonellini and Aydin,
321 1995](#); [Borg et al., 1960](#); [Engelder, 1974](#); [Knipe, 1989](#)). During the process of
322 cataclasis, the porosity and permeability are reduced because the cataclasis

323 results in the collapse of porosity and the reduction of grain size (Fisher and
324 Knipe, 1998). Rawling and Goodwin (2003) also suggests that cataclasis
325 presents different micro-deformation mechanisms depending on the burial
326 depth, i.e., cataclasis in sediments at shallow depths is dominated by grain
327 spalling and flaking whereas cataclasis at deeper depths is primarily
328 characterized by transgranular fracturing and grain crushing. The grain-
329 sorting within cataclasites is becoming poorer by grain fracturing and
330 chipping at early stage, and the following predominant chipping and crushing
331 then enhance the grain sorting. As an effective tool to study the cataclasis
332 processes of fault rocks, micro-structural analysis has been utilized in many
333 case studies (Antonellini et al., 1994; Blenkinsop, 1991; Fisher and Knipe,
334 1998; Jolley et al., 2007b; Tueckmantel et al., 2010), suggesting that the
335 concentration of clay/phyllosilicate materials in host rocks can inhibit the
336 probability of occurrence of cataclasis. Therefore, the sandstones with high
337 clay/phyllosilicate content are likely to be resistant to the cataclasis during
338 faulting deformation, as the clay/phyllosilicate-rich sandstones tend to
339 deform more easily by grain sliding and rotation rather than by grain
340 fracturing. However, different textures of impure sandstones (e.g., the
341 distribution of clay/phyllosilicate minerals) also affect the modalities of
342 cataclastic deformation.

343 **4.4. Diffusive Mass Transfer by Pressure Solution and Quartz**

344 **Cementation**

345 Diffusive mass transfer, a process of mass transfer from high-pressure sites
346 to low-pressure sites, happens when materials are dissolved at the grain
347 contacts and then transported by diffusion to free pore spaces where the

348 dissolved materials reprecipitate (Fisher and Knipe, 1998; Fisher et al., 2009;
349 Fossen et al., 2007; Knipe et al., 1997; Rutter, 1983; Spiers and Schutjens,
350 1990). Diffusive mass transfer is actually a redistribution of soluble materials
351 from their original sites with high pressure, by means of dissolution, transport
352 and reprecipitation (Dewers and Ortoleva, 1990; Fisher et al., 2009; Knipe et
353 al., 1997; Tueckmantel et al., 2010); and can alter the porosity and
354 permeability of fault rocks.

355 Based on the micro-structural analysis, it is found that the extent of diffusive
356 mass transfer is dominated by the clay/phyllsilicate content and its
357 distribution at the time of deformation (Fisher and Knipe (1998); Fisher and
358 Knipe, 2001; Fossen et al., 2007; Tueckmantel et al., 2010). For example: (i).
359 for clean sandstones with clay/phyllsilicate contents of <5%, the fault zones
360 experience enhanced quartz cementation within fault zones but can occur
361 with no enhanced pressure solution (i.e. an external source is involved); (ii).
362 for clean sandstones with higher clay/phyllsilicate content of 5-15%, there
363 is evidence for both enhanced pressure solution and quartz cementation (i.e.
364 an internal source is involved); (iii). for impure sandstones with
365 clay/phyllsilicate contents of 15-25%, the fault zones can experience
366 enhanced pressure solution but no extensive enhanced quartz cementation;
367 (iv). for impure sandstones with clay/phyllsilicate content of >25%, the
368 porosity and permeability of the fault zones may not be significantly affected
369 by either pressure solution or quartz cementation. The reason for these
370 observations is that diffusive mass transfer needs a catalyst
371 (clay/phyllsilicate) for pressure solution as well as nucleation sites for
372 quartz cementation. The rate of diffusive mass transfer is especially

373 determined by the presence and distribution of clay/phylosilicate. For
374 example, the presence of small concentration of clay/phylosilicate minerals
375 at the grain-contact points promotes the occurrence of pressure solution (e.g.
376 Odling et al., 2004); while clay/phylosilicate-coating on the quartz grains
377 inhibits the quartz cementation (e.g. Tada and Siever, 1989), because the
378 coating clay/phylosilicate minerals reduce the effective surface area of
379 quartz grains available for precipitation.

380 **4.5. Porosity Reduction by Disaggregation and Mixing**

381 In this fault seal process, there is no extensive grain fracturing but just
382 disaggregation and mixing of grains by means of particulate flow (Rawling
383 and Goodwin, 2003; Rawling and Goodwin, 2006), e.g., grain rolling and
384 grain sliding, which means this process results in the reorganisation of
385 distribution of detrital grains and clay/phylosilicate minerals without a
386 universal reduction of grain size (Fisher and Knipe, 1998; Fossen et al.,
387 2007; Knipe et al., 1997; Ottesen Ellevset et al., 1998). This fault process is
388 common in sedimentary units that are unconsolidated or unlithified, as in this
389 situation there is enough space for grains and clay/phylosilicate minerals to
390 be redistributed during faulting deformation (Bense et al., 2003; Fisher and
391 Knipe, 1998; Fossen et al., 2007; Knipe et al., 1997; Ottesen Ellevset et al.,
392 1998). The sedimentary units that are buried at shallow depths tend to
393 experience disaggregation and mixing to reduce the rock porosity. The
394 distribution of both detrital grains and clay/phylosilicate minerals can be
395 heterogeneous when initially deposited and then becomes more
396 homogeneous after the disaggregation and mixing during faulting
397 deformation, thus altering permeability pathways.

398 The permeability of fault rocks produced by disaggregation and mixing
399 varies within a big range, depending on the clay/phyllsilicate content of the
400 host rocks (Fisher and Knipe, 1998; Knipe et al., 1997). Furthermore, it is
401 suggested that disaggregation can result in either an enhancement or a
402 reduction of porosity, which depends on whether the disaggregation zone
403 has a dilational or compactional component (Fossen and Bale, 2007; Fossen
404 et al., 2007; Fossen et al., 2011). For clean sandstones, because the grain
405 size and grain sorting of the fault rock do not change considerably after the
406 reorganization of detrital grains, the fault rock porosity and permeability are
407 not changed significantly. In contrast, for impure sandstones, as well as the
408 reorganization of detrital grains, the fine-grained clay/phyllsilicate minerals
409 are also mixed with these detrital grains, resulting in the occupation of micro-
410 porosity between the detrital grains by the fine-grained clay/phyllsilicate
411 minerals. In this scenario, barriers for fluid flow can be produced and the
412 sealing capacity is effectively increased. Although Fisher and Knipe
413 observed a permeability reduction of up to one order of magnitude in
414 phyllsilicate-bearing disaggregation zones (Fisher and Knipe, 2001),
415 disaggregation zones generally have very limited effects on the permeability
416 of sandstone reservoirs as the permeability contrast is relatively low (Fossen
417 et al., 2007).

418 **5. Fault rock classification**

419 Fisher and Knipe (2001) suggested that fluid flow properties of faults are
420 significantly influenced by the presence of clay/phyllsilicate in three ways:
421 (i). the high concentrations of clay/phyllsilicate can produce fault rocks
422 within which most of the original porosity is occupied by the fine grained

423 clay/phylosilicate minerals and the micro-porosity (Fisher and Knipe, 1998);
424 (ii). there is a higher potential for clay/phylosilicate smearing within the
425 sedimentary units with high clay/phylosilicate contents (Lindsay et al., 1993);
426 and (iii). the existence of clay/phylosilicate materials between framework-
427 silicate grains promotes pressure solution and quartz cementation (Fisher
428 and Knipe, 1998). Therefore, if the faults maintain self-juxtaposition of these
429 units, the fault rock types related to the fault rock seals can be classified
430 according to the composition (especially the clay/phylosilicate content) of
431 the host rocks from which the fault rocks are produced. Where faulting
432 exceeds the thickness of the host units, the resulting clay content of the fault
433 rock (from smearing and mixing of the host rocks involved in the faulting),
434 grain size reduction processes and the potential for cementation can impact
435 on the fault rock flow properties.

436 Fault rocks can therefore be classified into the following groups (Fisher et al.,
437 2003; Fisher and Knipe, 1998; Fisher et al., 2009; Knipe et al., 1997;
438 Ottesen Ellevset et al., 1998): the cemented faults/fractures; the
439 clay/phylosilicate smears; the phyllosilicate-framework fault rocks (PFFRs);
440 the cataclasites; and the disaggregation zones (Fig.3). This classification is
441 based on the relationship between the clay/phylosilicate content and fault
442 rock types.

443 Fig.3 Illustration of typical fault rocks and their clay/phylosilicate contents,
444 showing the important control of the clay/phylosilicate content on the
445 fault rock development (modified from Ottesen Ellevset et al., 1998).

446 5.1. Cemented faults/fractures

447 Fault seal analysis based on the prediction of fault rock clay contents can be
448 invalidated if cemented fault zones are extensively developed (Fig.4) (Jolley
449 et al., 2007b; Knipe, 1993a; Knipe et al., 1997). However, in most cases, the
450 cementation is not extensive enough to influence the sealing properties of
451 the fault zones (Ottesen Ellevset et al., 1998), as the cementation can rarely
452 form continuous seals but is often restricted to limited areas of the fault zone
453 or between the footwall and the hanging wall cut offs of units prone to
454 cementation.

455 Fig.4 A schematic cartoon (modified from Jolley et al., 2007b) and a typical
456 micro-graph (Pei, 2013) of cemented faults/fractures. The cement seals
457 can occur when minerals' dissolution-reprecipitation process or new
458 minerals' precipitation dominate the sealing properties of
459 faults/fractures.

460 Generally, cement seals only happen in fault zones where the sealing
461 properties are dominated by the minerals' dissolution-reprecipitation process
462 or where new minerals' precipitation is promoted (Knipe, 1997). Therefore,
463 the cement seals are mostly associated with the sites where local dissolution
464 and reprecipitation happen during deformation or along the invasion paths of
465 fluids in the faults. For cemented faults and fractures, Knipe et al. (1997)
466 found that cementation is the dominant mechanism of porosity reduction
467 within the fault zones. There are probably two main sources of cements: the
468 local soluble minerals within the fault zones; and the invaded fluids along the
469 fault planes. Because of the high density of nucleation sites on the fault
470 planes, both the local soluble minerals and invaded fluids can be easily

471 precipitated along or adjacent to the fault planes. [Ottesen Ellevset et al.](#)
472 [\(1998\)](#) suggested that the cementation extent along the fault planes may be
473 limited to three times the thickness of the unit that acts as a source unit for
474 the cementation.

475 **5.2. Clay/Phyllosilicate Smears**

476 As shown in the fault rock classification (Fig.3), fault rocks with
477 clay/phyllosilicate contents >40% are defined as clay smears. These can
478 develop from the deformation of a host shale rock with >40%
479 clay/phyllosilicate content at the time of deformation ([Jolley et al., 2007b](#);
480 [Knipe, 1997](#); [Knipe et al., 1997](#); [Ottesen Ellevset et al., 1998](#)). In this
481 situation, a continuous clay material zone with low-permeability along fault
482 planes can be produced during the faulting deformation (Fig.5). The factors
483 controlling the clay/phyllosilicate smear continuity are the content and
484 distribution of clay/phyllosilicate-rich units, fault throw ([Bouvier et al., 1989](#);
485 [Fulljames et al., 1997](#); [Lindsay et al., 1993](#); [Yielding et al., 1997](#)), and the
486 lithification state ([Egholm et al., 2008](#); [Heynekamp et al., 1999](#); [Loveless et](#)
487 [al., 2011](#)). Based on the studies on the distribution of clay smears in Sleipner
488 Vest of North Sea ([Knipe, 1997](#); [Ottesen Ellevset et al., 1998](#)), it was
489 suggested that the clay/phyllosilicate smears often become discontinuous
490 once the fault throw is larger than three times the thickness of
491 clay/phyllosilicate-rich stratigraphic units.

492 Fig.5 A schematic cartoon ([modified from Jolley et al., 2007b](#)) and a typical
493 micro-graph ([Pei, 2013](#)) of clay/phyllsilicate smears, containing >40%
494 clay/phyllsilicate minerals. Clay smears can act as effective seals
495 when continuous clay material zones are produced along fault planes
496 during the faulting deformation.

497 **5.3. Phyllosilicate-framework fault rocks (PFFRs)**

498 As shown in the fault rock classification (Fig.3), phyllosilicate-framework fault
499 rocks (PFFRs) contain 15-40% clay/phyllsilicate minerals. These can
500 develop from impure sandstones containing 15-40% clay/phyllsilicate at the
501 time of deformation or from the mixing of high and low clay content units
502 ([Fisher and Knipe, 1998](#); [Jolley et al., 2007b](#); [Knipe, 1992a](#); [Knipe et al.,](#)
503 [1997](#)). An impure sandstone, with a mixture of phyllosilicates and framework
504 silicates, can produce PFFRs where the petrophysical properties are
505 dominated by the generation of anastomosing networks of the micro-smears
506 around the framework fragments or clasts (Fig.6) ([Knipe, 1997](#)). These
507 micro-smears may have similar properties to the clay smears; thus, as
508 pointed out by [Knipe \(1992a\)](#), it is not necessary to have clay units for
509 creating PFFRs if the sealing properties are determined by the continuity
510 and the structure of deformed phyllosilicates.

511 [Ottesen Ellevset et al. \(1998\)](#) pointed out that the occurrence of PFFRs has
512 great effects on the sealing behaviour in two areas, which are the area
513 where the impure sandstones directly juxtapose against the fault zones; and
514 the area along fault planes between the hanging wall and footwall cut-offs of
515 impure sandstone units. The latter scenario is to some extent similar to the
516 behaviour of clay/phyllsilicate smears. The continuity of the PFFRs

517 determines the effectiveness of PFFRs to form effective retarders for fluid
518 flow (Fisher and Knipe, 1998; Knipe et al., 1997; Ottesen Ellevset et al.,
519 1998).

520 Fig.6 A schematic cartoon (modified from Jolley et al., 2007b) and a typical
521 micro-graph (Pei, 2013) of phyllosilicate-framework fault rocks (PFFRs),
522 containing 15-40% clay/phyllosilicate minerals. The petrophysical
523 properties of phyllosilicate-framework fault rocks are dominated by the
524 generation of anastomosing networks of the micro-smears around the
525 framework fragments or clasts.

526 **5.4. Cataclasites**

527 Cataclasites dominate seal development in clean sandstones containing <15%
528 clay content at the time of deformation (Fisher and Knipe, 1998; Jolley et al.,
529 2007b; Knipe et al., 1997; Ottesen Ellevset et al., 1998). Because of the low
530 clay content within such host rocks, the main mechanisms of porosity and
531 permeability reduction are the cataclasis and the post-deformation quartz
532 cementation (Fisher and Knipe, 1998). During the process of cataclasis, the
533 grain size decreases by means of grain fracturing and frictional grain rolling,
534 resulting in the porosity reduction and potential cementation (Fig.7). The
535 frictional grain rolling lead to the irregular grains sub-parallelly aligned to the
536 shearing direction, which makes the compaction more easily to reduce the
537 fault rock porosity. The granulation seams or deformation bands, which are
538 discussed in many studies (Antonellini and Aydin, 1994; Knipe, 1992a; Knipe,
539 1993a; Knipe, 1993b), are examples of cataclasites.

540 Fig.7 A schematic cartoon (modified from Jolley et al., 2007b) and a typical
541 micro-graph (Pei, 2013) of cataclasites, containing <15%
542 clay/phyllsilicate minerals. The grain size reduction of cataclasites is
543 dominated by grain fracturing and frictional grain sliding, resulting in the
544 porosity reduction and potential cementation.

545 Previous research has pointed out that the permeability of cataclasites
546 varies over a large range; this depends on the lithification state of the host
547 rocks (Fisher and Knipe, 1998; Knipe et al., 1997). According to the
548 lithification state, the cataclasites can be divided into three types: (i). poorly
549 lithified cataclasites, which show little or even no compaction or cementation
550 (post-deformation) and point contacts are maintained between grains; (ii).
551 partially lithified cataclasites, which have some compaction and cementation;
552 and (iii). lithified cataclasites, which comprise grains interlocked by post-
553 deformation dissolution and/or cementation (Knipe, 1992a; Knipe, 1993b;
554 Knipe et al., 1997).

555 **5.5. Disaggregation Zones**

556 The disaggregation zones are fault rocks generated by deformation without
557 fracturing. They can also be produced from pure, low clay-content (<15%)
558 sandstones (Fig.3), similar to the generation of the cataclasites (Fisher and
559 Knipe, 1998; Fossen et al., 2007; Jolley et al., 2007b; Knipe et al., 1997;
560 Loveless et al., 2011; Ottesen Ellevset et al., 1998; Rawling and Goodwin,
561 2003). However, the host rocks of disaggregation zones are normally sands
562 or poorly consolidated sandstones (Bense et al., 2003; Rawling and
563 Goodwin, 2006). In the process of disaggregation, the grains move by way
564 of particulate flow (Rawling and Goodwin, 2003) to accommodate the strain

565 during faulting deformation, with no extensive grain fracturing (Fisher and
566 Knipe, 1998; Knipe et al., 1997). The permeability of disaggregation zones is
567 usually higher than that of the other types of fault rocks. It is difficult for
568 disaggregation to form effective seals to prevent fluid flow, because there
569 are not sufficient clays/phyllosilicates within the disaggregation zones to act
570 as a source for either the cementation or the clay/phyllosilicate smears
571 (Fisher and Knipe, 2001; Fossen et al., 2007) (Fig.8).

572 Fig.8 A schematic cartoon (modified from Jolley et al., 2007b) and a typical
573 micro-graph (Knipe et al., 1997) of disaggregation zones.
574 Disaggregation zones are developed in poorly lithified rocks containing
575 <40% clay/phyllosilicate minerals. As there is not sufficient
576 clays/phyllosilicates, disaggregation zones cannot form effective seals
577 for fluid flow under normal conditions.

578 Based on this fundamental fault rock classification, Fisher and Knipe (1998)
579 constructed the relationship between a wide spectrum of fault rocks with
580 different geological settings, including clay content, degree of fragmentation
581 and lithification state (Fig.9). This detailed fault rock classification allows
582 geologists to make basic prediction of fault rock types (siliciclastic rocks, e.g.,
583 sandstones, siltstones, mudstones and shales) and properties by
584 considering clay content, degree of fragmentation and lithification state.

585 Fig.9 Diagram showing different types of fault rocks developed in the North
586 Sea and their relationship to the composition of the host sediment and
587 the extent of grain-size reduction and post-deformation lithification
588 experienced (Fisher and Knipe, 1998).

589 **6. Methods to evaluate fault sealing properties**

590 In the recent 20 years, geologists have developed and used several
591 methods to evaluate the fault sealing properties. The i) Allan map, ii) triangle
592 juxtaposition diagram and iii) clay smear indices can be employed to
593 evaluate the fluids flow properties for juxtaposition sealing faults, while the
594 micro-structural analysis and petrophysical assessment can be used to
595 investigate the fluids flow properties for fault rock sealing faults (Table 1).
596 The production simulation modelling also has been employed to predict the
597 petroleum migration and accumulation features, including consideration of
598 fault zone compartmentalization and its hydrocarbon sealing behaviour (e.g.,
599 [Fachri et al., 2013b](#); [Fisher and Jolley, 2007](#); [Manzocchi et al., 2002](#);
600 [Manzocchi et al., 1999](#); [Ottesen Ellevset et al., 1998](#); [Zijlstra et al., 2007](#)).
601 Although all these methods have their own shortcomings, the methods have
602 been improved to become more and more effective and useful for evaluation
603 of the fault sealing properties.

604 Table 1 A summary of the methods to evaluate fault sealing properties for
605 different fault seal classifications.

606 **6.1. Stratigraphic juxtaposition methods**

607 [Allan \(1989\)](#) introduced a model to relate faults to hydrocarbon migration
608 and entrapment, suggesting the influence of faults on the hydrocarbon
609 migration and the entrapment is determined by the lithology of juxtaposed
610 stratigraphic units on different sides of fault and the fault throws between the
611 hanging wall and the footwall cut-offs. The model provides a 3D overview
612 and understanding on the architecture of the fault juxtapositions, the

613 stratigraphic units and the fault throws, which can help to understand the
614 stratigraphic contacts, the fault geometry and the structure/closure style.

615 [Knipe \(1997\)](#) presented an effective technique of triangle juxtaposition
616 diagram, which can be used to quickly judge what types of fault seals can be
617 formed based on the resultant stratigraphic juxtapositions between the
618 hanging wall and footwall (Fig.10). The Fig.10 illustrates the use of sidewall
619 charts to review the key host rock characteristics. These variables control
620 the development of fault rocks and seals. This example shows depth plots of
621 the host rock properties, porosity, permeability, percentage of phyllosilicate
622 (abbreviated “Phyllo” in the key) laminations present, and the net/gross
623 ratios.

624 It is known that reservoir stratigraphic units (e.g., permeable sandstones)
625 juxtaposing against impermeable stratigraphic units (with high concentration
626 of clay/phyllosilicate materials, e.g., shales/mudstones) probably form fault
627 seals; while leaking windows are more likely if reservoir sand stratigraphic
628 units are juxtaposed against each other. By using the triangle juxtaposition
629 diagram, it is possible to make an initial judgement and prediction of fault
630 sealing properties, particularly when seeking possible leaking windows.
631 Moreover, in the triangle juxtaposition diagram, the sidewall charts can also
632 be attached to provide more details of the stratigraphy, such as the sand
633 net/gross ratio, the clay/phyllosilicate content, the host rock lithology and the
634 host rock permeability (e.g., [Cervený et al., 2004](#); [Knipe, 1997](#); [Knipe et al.,](#)
635 [1997](#)). These details contribute to allow a more reliable assessment and
636 prediction of sealing properties on the faults. Different types of juxtapositions
637 between different stratigraphic units can be identified on this diagram; and

638 these different juxtaposition types provide important clues for estimating the
639 fault sealing properties of different places on the fault plane with various fault
640 throws.

641 Fig.10 The triangle juxtaposition diagram uses sidewall chart input to identify
642 the leaking windows and the fault seals resulting from the stratigraphic
643 juxtapositions between the hanging wall and the footwall (Knipe, 1997).
644 The juxtaposition diagram key lists the different types of important
645 juxtapositions that occur on different parts of the fault plane and
646 contribute to the fluid flow behavior of faults with different throw
647 magnitudes. Note that the throws associated with the development of
648 an area of high-permeability sand juxtaposed against high-permeability
649 sand (red area) can be rapidly identified.

650 A 3D numerical model of fault displacement, proposed by Clarke et. al.
651 (2005), enables the building of geological models to represent the complex
652 3D geometry and geological properties of a fault, which can be employed to
653 predict the cross-fault juxtaposition relationships in 3D space. The further
654 forward modelling of fault development allows a 4D prediction of fault
655 juxtaposition (with time). The successful application in the Artemis Field
656 (Southern North Sea, UK) and the Moab Fault (Utah, USA) demonstrates
657 significant improvements in the 3D and 4D prediction of fault juxtaposition
658 seals for both a single fault and multiple faults.

659 **6.2. Clay smear indices**

660 Bouvier et al. (1989) employed Clay Smear Potential (CSP) to estimate the
661 potential of occurrence of clay smearing based on studies of three-
662 dimensional seismic interpretation and fault sealing investigations in Nun

663 River field in Nigeria. The CSP represents the relative amount of clay (e.g.,
664 mudstones, shales, etc.) that has been smeared from individual shale
665 source beds at a certain point along a fault plane during faulting deformation.
666 The CSP was then expressed more explicitly by [Fulljames et al. \(1997\)](#)
667 (Fig.11a). The CSP represents the total amount of clay/phyllsilicate that
668 has been smeared from every stratigraphic unit with high clay/phyllsilicate
669 content along the fault planes. The value of CSP increases with increasing
670 thickness of shale/mudstone beds and the number of stratigraphic units with
671 high concentrations of clay/phyllsilicate, and the CSP decreases with
672 increasing fault throw.

$$\text{CSP} = \sum \frac{(\text{Shale bed thickness})^2}{\text{Distance from source bed}}$$

673 [Lindsay et al. \(1993\)](#) introduced Shale Smear Factor (SSF, Fig.11b) to
674 estimate the magnitude of fault seals formed by smearing of
675 clay/phyllsilicate-rich units, e.g., shales and mudstones. The SSF value is
676 proportional to the fault throws and inversely proportional to the thickness
677 and the number of source units of clay/phyllsilicate. Using the SSF
678 algorithm to estimate the extent of clay/phyllsilicate smears, there is
679 increasing potential to form a continuous clay/phyllsilicate smears with
680 increasing thickness and number of source unites of clay/phyllsilicate and
681 decreasing fault throws, and vice versa.

$$\text{SSF} = \frac{\text{Fault throw}}{\text{Shale layer thickness}}$$

682 The Shale Gouge Ratio (SGR, Fig.11c) was proposed ([Yielding et al., 1997](#))
683 to estimate the clay content in faults from the mixing of units with different
684 clay contents in the throw interval. This helps evaluate fault seals in more

685 complex stacking sequences. The SGR is proportional to cumulative
686 thickness of shale beds within a scale of a distance equal to fault throw and
687 inversely proportional to fault throw.

$$\text{SGR} = \frac{\sum(\text{Shale bed thickness})}{\text{Fault throw}} \times 100\%$$

688 Furthermore, the definition of SGR was extended for a package of
689 sediments (Fig.11d). In this situation, SGR is considered to be the
690 percentage of clay present in all units in the throw interval.

$$\text{SGR} = \frac{\sum[(\text{Zone thickness}) \times (\text{Zone clay fraction})]}{\text{Fault throw}} \times 100\%$$

691 The CSP and SSF estimate the fault sealing properties by considering the
692 continuity of smearing of shale/mudstone beds; while the SGR calculates the
693 average mixture of clays likely to be present at different point on a fault.

694 Fig.11 Diagram and calculation of methods for estimation of fault seals
695 (especially fault seals formed by clay/phyllsilicate smearing): (a) Clay
696 Smear Potential (CSP) (Bouvier et al., 1989; Fulljames et al., 1997); (b)
697 Shale Smear Factor (SSF) (Lindsay et al., 1993); (c, d) Shale Gouge
698 Ratio (SGR) (Yielding et al., 1997).

699 **6.3. Microstructural analysis**

700 As introduced above, the fault rocks are generated when the sedimentary
701 units are entrained into the fault zones. The detailed evaluation of different
702 types of fault rocks can be achieved by integrating micro-structural analysis
703 on the deformation mechanisms and the porosity and permeability data. The
704 Scanning Electron Microscope (SEM) was employed in Knipe (1992a) to
705 investigate the micro-structures of fault rocks. The following studies (e.g.,

706 Fisher et al., 2003; Fisher and Knipe, 1998; Fisher and Knipe, 2001; Fisher
707 et al., 2009; Ottesen Ellevset et al., 1998; Rawling and Goodwin, 2003;
708 Tueckmantel et al., 2010) integrated the fault rock petrophysical sealing
709 properties with the micro-structural analysis on the fault rocks developed
710 within the fault zones.

711 Fig.12 The sample photo and BSE micrographs showing the PFFRs
712 developed in impure sandstones (Pei, 2013).

713 The micro-structural analyses undertaken are laboratory based that aim to
714 characterise the microstructures and the petrophysical properties of fault
715 rocks and compare these to their host rocks, in order to estimate the
716 deformation mechanisms and the fault seal processes that the fault rocks
717 experienced, and to identify the relative timing of deformation during
718 diagenesis. For example, Fig.12 presents the BSE micrographs of a fault
719 rock sample from northern Qaidam basin in China (Pei, 2013). The sample
720 is located within the fault zone of the fault outcrop, comprising fine-grained
721 impure sandstone (7-13% clay content) as the dominated lithology. A series
722 of PFFRs (20-35% clay content) are formed in the shear zones or
723 deformation bands. The grain size experiences small reduction in the fault
724 rocks. The BSE micrographs demonstrate the relative high content of fine-
725 grained phyllosilicates, strong pressure solution and low porosity in the fault
726 rocks when compared to the surrounding host rocks.

727 **6.4. Petrophysical assessment**

728 The petrophysical properties of the fault rocks have been measured to
729 evaluate the sealing capacity of the fault rocks quantitatively in many
730 previous studies (e.g., Fisher and Knipe, 1998; Fisher and Knipe, 2001;

731 [Jolley et al., 2007b](#); [Ottesen Ellevset et al., 1998](#); [Tueckmantel et al., 2010](#)).
732 A case study in the North Sea and Norwegian Continental Shelf plotted the
733 permeability of fault rocks against the clay content of the host rocks for
734 various fault rock types ([Fig.13](#)) ([Fisher and Knipe, 2001](#)). The case study
735 suggests that for low throw faults with self-juxtaposition, the clean
736 sandstones (clay content <15%) tend to form cataclasites that do not always
737 represent effective fluid flow barriers; the impure sandstones (clay content
738 15%-40%) experience significant porosity and permeability reduction; while
739 the mudstones or shales form continuous clay smears with very low
740 permeability that can be effective barriers for fluid flow across the fault
741 zones. It also highlights that the permeability of the fault rocks is not only
742 determined by the clay content of host rocks, but also related to their burial
743 history ([Fig.13](#)). Different burial history implies that fault rocks have
744 experienced different stress and temperature during fault deformation, which
745 results in variable range of permeability of fault rocks. Therefore, the
746 petrophysical assessment of fault rocks becomes an effective method to
747 provide reliable poroperm results for the evaluation of fault sealing capacity.

748 Fig.13 Summary of the fault rock permeability from the North Sea and
749 Norwegian Continental Shelf ([modified from Fisher and Knipe, 2001](#)).
750 The permeability of various fault rocks is plotted against the clay
751 content of the host rocks. The chart also describes the control of the
752 burial depth at the time of faulting and maximum post-deformation
753 burial depth on the fault rock permeability.

754 **6.5. Production simulation modelling**

755 Production simulation modelling is an effective tool to predict the petroleum
756 migration and accumulation characteristics in petroleum industry in the last
757 decades. The accurate input of geologic data into the simulation model,
758 particularly the data of fault zone architecture and fault rock properties, is
759 vital to increase the confidence in the reliability of its predictive capability.
760 Based on a series of case studies ([Fisher and Jolley, 2007](#); [Harris et al.,](#)
761 [2007](#); [Jolley et al., 2007b](#); [Zijlstra et al., 2007](#)), [Fisher and Jolley \(2007\)](#)
762 proposed several advices for those who would like to incorporate the effects
763 of fault architecture on fluid flow in a production simulation model.

764 i) A geometrically accurate structural interpretation should not get compromised
765 during transfer and incorporation into the production simulation model,
766 particularly the fault zone geometry and fault compartmentalization.

767 ii) The transmissibility multipliers should be calculated based on realistic fluid
768 flow properties of the fault rocks obtained within the field.

769 iii) Apart from single-phase permeability of the fault rocks, it is also of
770 importance to consider the capillary pressure and relative permeability in some
771 situation, particularly for high net: gross reservoirs with cataclastic fault rocks
772 developed within the fault zone ([Al-Busafi et al., 2005](#); [Manzocchi et al., 2002](#)).

773 iv) As the interpretation of the data is often non-unique, caution must be given
774 when concluding what the data actually reveal about fault-related fluid flow, in
775 order to decrease the uncertainties being introduced into the production-related
776 fault seal analysis.

777 The concept of 'fault facies' has also been proposed to define any features
778 deriving its present properties from tectonic deformation, which can improve

779 the understanding the impact of fault zone architecture on hydrocarbon
780 sealing behaviour (Tveranger et al., 2004; Tveranger et al., 2005). Originally,
781 the concept of 'facies' is normally used to describe sedimentary rocks or
782 metamorphic rocks. The introduction of fault facies allows the natural
783 extension of the facies concept into the realm of both fault zone architecture
784 and its fault rock properties (Braathen et al., 2009). As fault facies are
785 associated to the fault geometry, internal structure, petrophysical properties
786 and fault spatial distribution, it provides a novel approach to incorporate fault
787 zone architecture and its impact on fluid flow properties into a three-
788 dimensional production simulation model (Braathen et al., 2009; Fachri et al.,
789 2013b; Fachri et al., 2011; Manzocchi et al., 2010).

790 **7. Factors affecting petrophysical properties of fault rocks**

791 The petrophysical properties of fault rocks are mainly determined by the
792 clay/phyllosilicate content, the level of cataclasis and the amount of
793 cementation (Fig.9) (Fisher and Knipe, 2001). However, in some natural
794 oil/gas fields, the fault rocks, generated from sandstones with identical
795 clay/phyllosilicate contents, can have different porosity and permeability
796 characteristics (e.g. Fisher et al., 2003; Fisher and Knipe, 2001; Fossen et
797 al., 2007). Based on a case study on the cataclastic faults from the
798 Rotliegendes of the Southern North Sea, this can be attributed to the burial
799 history that leads to interaction between the temperature history and the
800 stress history (Fig.14), which can alter the petrophysical properties of fault
801 rocks within the fault zones (Fisher and Knipe, 2001). For example, faults
802 within the Rotliegendes formed at deeper depths than that in the Middle
803 Jurassic reservoirs and therefore are closer to the temperature at which

804 quartz precipitates rapidly (Fig.14). Apart from temperature and stress
805 history, geological time is a third factor influencing the permeability evolution
806 of a fault zone, which means a same fault zone can present different sealing
807 properties through geological time ([Indrevær et al., 2014](#)).

808 Fig.14 Data of cataclastic faults from the Rotliegendes of the Southern North
809 Sea. The plots show (a) permeability against their maximum burial
810 depth and (b) permeability contrast against their maximum burial depth
811 ([Fisher and Knipe, 2001](#)).

812 **7.1. Temperature history**

813 It has been commonly accepted that the temperature history of fault rocks
814 has a significant effect on the rate of meso-diagenesis, e.g., quartz
815 cementation and pressure solution ([Walderhaug, 1996](#)). The rate usually
816 increases as a function of temperature ([Fisher et al., 2003](#); [Fisher and Knipe,](#)
817 [2001](#); [Fisher et al., 2009](#)), e.g., the quartz cementation and pressure solution
818 occurs at rapid rate when the temperature exceeds ~90 °C.

819 **7.2. Stress History**

820 Many studies tried to identify the effects of confining pressure on the
821 deformation behaviour of faults/fault zones in sandstones. These studies
822 suggest that: the sandstones at low confining pressures are likely to
823 experience brittle faulting (failure occurs along single slip planes), while the
824 sandstones at high confining pressures prefer more distributed ductile
825 deformation without the generation of discrete slip planes (e.g. [Handin et al.,](#)
826 [1963](#); [Scott and Nielsen, 1991](#)). The experimental studies indicate that the
827 grain size and the permeability of faults/fault zones decrease with increasing

828 confining pressure and temperature (e.g. Crawford, 1998; Engelder, 1974;
829 Fisher and Knipe, 2001; Zhu and Wong, 1997).

830 Therefore, as well as the clay/phyllsilicate content of host rocks, the effects
831 of temperature history and stress history need to be taken into account when
832 evaluating the fault sealing properties (Fisher et al., 2003; Fisher and Knipe,
833 2001; Fossen et al., 2007; Jolley et al., 2007b). The schematic cartoons in
834 Fig.15 demonstrate the potential effects of burial depth (increasing effective
835 stress and temperature) on micro-structural deformation mechanisms (Jolley
836 et al., 2007b). Firstly, the different fault seal processes do not always occur
837 independently, and it is common to observe multiple fault seal processes in
838 a same fault zone. Secondly, the occurrence of combinations of fault seal
839 processes is determined by both the clay/phyllsilicate content and the burial
840 depth, as these two factors control the clay/phyllsilicate content of the
841 generated fault rocks and its deformation environment (stress &
842 temperature).

843 Fig.15 Schematic cartoons of micro-structural deformation mechanisms with
844 various fault rocks generated in different geological settings, e.g., clay
845 content of the host rocks and burial depth (reflecting increasing
846 effective stress and temperature) (modified from Jolley et al., 2007b).

847 **7.3. Cyclic evolution of permeability through geological time**

848 As a same fault zone can present different hydrocarbon sealing behaviour
849 through geological time, it is of importance to understand the control of
850 geological time on the permeability evolution of a fault zone (both cross and
851 along a fault zone). Many studies, particularly on production simulation
852 modelling, have investigated the role of geological time on fault zone

853 permeability evolution (Fisher and Knipe, 2001; Indrevær et al., 2014; Jolley
854 et al., 2007b; Knipe et al., 1997; Manzocchi et al., 2010; Manzocchi et al.,
855 2002). Indrevær et. al. (2014) proposed a model to demonstrate the cyclic
856 permeability evolution of fault zones through geological time (Fig.16),
857 describing faults as (i) conduits, (ii) barriers or (iii) conduits and barriers
858 under different circumstances. At stage (a), the fault zone acts as fluid
859 conduits as the porosity and permeability are increased by fracturing and
860 cataclasis during faulting deformation. At stage (b), after the faulting
861 deformation, the fault core zone acts as barriers whereas the damage zone
862 acts as conduits for fluid flow, as the following precipitation of minerals and
863 grain growth within the fault core zone inhibit the fluid flow. At stage (c), the
864 entire fault zone is sealed by further grain growth and precipitation
865 processes through time, and therefore acts as barriers for fluid flow, both
866 along and across fault zone. At stage (d), a new permeability evolution cycle
867 of the fault zone is restarted when the fault zone is reactivated in a later
868 faulting deformation. Although this schematic permeability evolution model
869 oversimplified many details associated with fault zone architecture and fault
870 sealing properties, it reveals a basic cyclic changes of leakage and sealing
871 across or along a fault zone through geological time.

872 Fig.16 Schematic illustration of a model showing the cyclic permeability
873 evolution of fault zones through geological time (modified from
874 [Indrevær et al., 2014](#)). (a) With faulting deformation, movement along a
875 fault causes fracturing and cataclasis within the core zone and
876 increases permeability. The core zone thereby acts as a fluid conduit.
877 (b) Precipitation of minerals and grain growth within the core zone
878 decreases permeability within the core zone and forces fluid flow into
879 the damage zone. (c) Further grain growth and precipitation processes
880 through time decrease porosity and permeability to gradually seal the
881 entire fault zone. (d) Fault reactivation will initiate a new fluid flow
882 evolution cycle.

883 **8. Limitations and future of fault seal analysis**

884 Fault seal analysis has been evolved since the concept of 'sealing' and 'non-
885 sealing' was proposed by Smith in 1966 ([Smith, 1966](#)). In the past 50 years,
886 by understanding the fault zone architecture, fault seal types, fault seal
887 processes and generated fault rocks, geologists have proposed a bunch of
888 models and methods to evaluate the hydrocarbon sealing behaviour of a
889 fault zone. The initial application of Allan map ([Allan, 1989](#)) and triangle
890 juxtaposition diagram ([Knipe, 1997](#)) makes it possible to investigate the
891 effects of stratigraphic juxtaposition on the fluid flow properties of a fault
892 zone. The later utilization of clay smear indices allows the quantitative
893 evaluation of fault sealing capacity ([Bouvier et al., 1989](#); [Fulljames et al.,](#)
894 [1997](#); [Lindsay et al., 1993](#); [Yielding et al., 1997](#)). The recent employment of
895 SEM photography and petrophysical assessment enables the investigation
896 of deformation mechanisms of fault rocks and their effects on grain size

897 reduction, porosity collapse and permeability decrease (e.g., Fisher et al.,
898 2003; Fisher and Knipe, 1998; Fisher and Knipe, 2001; Fisher et al., 2009;
899 Ottesen Ellevset et al., 1998). These methods have significantly boosted the
900 fault seal related analysis in the past decades; however, there is still great
901 potential for further progress in fault seal related research. The apparent
902 limitations of the present-day models/methods have significantly constrained
903 the effectiveness of fault seal analysis, such as:

904 a). Each individual model/method in present-day mostly focuses on a
905 certain scale, which inhibits the 'extrapolation' of the results to a
906 larger or smaller scale. A scale-dependent model/method may
907 overlook the characteristics at its own scale while neglect that at other
908 scales.

909 b). Further investigation and case studies are still necessary, as the
910 present models/methods have not been sufficiently validated by
911 physical simulation. The stratigraphic/mechanical heterogeneity
912 contributes to high degree of fault zone complexity; therefore, the
913 physical simulation is of great importance to validate the effectiveness
914 of fault seal evaluation using present models/methods.

915 c). The present methods of fault seal analysis are mostly used to
916 study the fault zone architecture and fault sealing properties in
917 extensional regimes. Many case studies have realized that
918 faults/fractures can play important control on the hydrocarbon
919 migration in contractional regimes, e.g., the study in Kentucky, USA
920 (Lewis et al., 2002), the New Guinea Fold Belt (Hill et al., 2004), the
921 North West Borneo (Ingram et al., 2004), the Qaidam basin (Pang et

922 al., 2004), etc. However, the detailed thrust fault architecture
923 (particularly the meso- to micro-scale deformation features) and its
924 effect on the fault sealing behaviour have not been well studied in
925 contractional systems.

926 d). The concept of 'fault facies', associated to the fault geometry,
927 internal structure, petrophysical properties and fault spatial
928 distribution, is apparently an effective approach for incorporating both
929 fault zone architecture and its impact on fluid flow properties into a
930 three-dimensional production simulation model. However, further
931 studies on fault facies are necessary to find how to apply this concept
932 in different geological settings.

933 Considering the limitations of present fault seal analysis methods, there are
934 a number of general paths to improve the fault seal analysis, for instance:

935 a). Multi-approach/scale investigation should be the direction for
936 further fault seal analysis. The results from an individual
937 model/method, however good, is of much less value if it was highly
938 scale-dependent. The multi-approach/scale fault seal analysis can
939 avoid the scale-limitation of the results.

940 b). Further fluid flow physical simulation of fault zones could be
941 employed to validate the fault seal analysis using the existing
942 models/methods. Fluid flow physical simulation can be an effective
943 'ground-truthing' tool to discriminate these models/methods as to their
944 accuracy of prediction in particular natural fault zones. A
945 model/method can be an effective model/method only if it was
946 sufficiently tested by 'ground-truthing' tools.

947 c). Fault seal analysis in contractional systems should be taken into
948 account. It is of great value to understand the differences of fault
949 sealing properties between contractional and extensional regimes,
950 particularly in the aspects of fault architecture, fault seal processes
951 and their effects on fluid flow properties.

952 d).Fault facies should be integrated into the production simulation
953 model to predict the impact of fault architecture on hydrocarbon
954 sealing behaviour within a fault zone.

955 **9. Conclusions**

956 Fault sealing properties is one of the most important aspects of fault zone
957 associated research. By understanding the fault zone architecture, fault seal
958 types, fault seal processes and generated fault rocks, geologists have
959 proposed different models and methods to evaluate the hydrocarbon sealing
960 behaviour of a fault zone in the past decades. The proposal of these
961 models/methods has significantly promoted the application of fault seal
962 analysis to natural fault zones.

963 The present models/methods have clearly enhanced the understanding of
964 fault zone sealing behaviour; however, further fault seal analysis should
965 consider multi-approach/scale and physical simulation, in both extensional
966 and contractional regimes.

967 **Acknowledgements**

968 It is impossible to finish this manuscript without the discussion and
969 suggestions from many colleagues over recent years. We would like to thank
970 Dr J. Geoff Lloyd, Dr Jonathan Imber, Dr Anren Li, Dr Henry Lickorish, and

971 Prof Xin Wang for the good communications contributing to this review
972 article. The constructive comments and suggestions from both the editor (Dr.
973 Carlo Doglioni) and two reviewers (Dr. Fabrizio Agosta and Dr. Kim Senger)
974 are of great use to this work and greatly appreciated. This work has been
975 collaboratively supported by the Fundamental Research Funds for the
976 Central Universities (15CX02004A), Shandong Provincial Natural Science
977 Foundation China (2014BSE28008, ZR2012DM011) and National Natural
978 Science Foundation of China (41272142).

979 **References**

- 980 Agosta, F., Ruano, P., Rustichelli, A., Tondi, E., Galindo-Zaldívar, J. and
981 Sanz de Galdeano, C., 2012. Inner structure and deformation
982 mechanisms of normal faults in conglomerates and carbonate
983 grainstones (Granada Basin, Betic Cordillera, Spain): Inferences on
984 fault permeability. *Journal of Structural Geology*, 45(0): 4-20.
- 985 Al-Busafi, B., Fisher, Q.J. and Harris, S.D., 2005. The importance of
986 incorporating the multi-phase flow properties of fault rocks into
987 production simulation models. *Marine and Petroleum Geology*, 22(3):
988 365-374.
- 989 Allan, U.S., 1989. Model for Hydrocarbon Migration and Entrapment within
990 Faulted Structures. *American Association of Petroleum Geologists
991 Bulletin*, 73(7): 803-811.
- 992 Antonellini, M. and Aydin, A., 1994. Effect of Faulting on Fluid-Flow in
993 Porous Sandstones - Petrophysical Properties. *American Association
994 of Petroleum Geologists Bulletin*, 78(3): 355-377.
- 995 Antonellini, M. and Aydin, A., 1995. Effect of Faulting on Fluid-Flow
996 Geometry and Spatial-Distribution. *American Association of
997 Petroleum Geologists Bulletin*, 79(5): 642-671.
- 998 Antonellini, M.A., Aydin, A. and Pollard, D.D., 1994. Microstructure of
999 deformation bands in porous sandstones at Arches National Park,
1000 Utah. *Journal of Structural Geology*, 16(7): 941-959.
- 1001 Aydin, A. and Eyal, Y., 2002. Anatomy of a normal fault with shale smear:
1002 Implications for fault seal. *Aapg Bulletin-American Association of
1003 Petroleum Geologists*, 86(8): 1367-1381.
- 1004 Balsamo, F., Storti, F., Salvini, F., Silva, A.T. and Lima, C.C., 2010.
1005 Structural and petrophysical evolution of extensional fault zones in
1006 low-porosity, poorly lithified sandstones of the Barreiras Formation,
1007 NE Brazil. *Journal of Structural Geology*, 32(11): 1806-1826.
- 1008 Bense, V., Van den Berg, E. and Van Balen, R., 2003. Deformation
1009 mechanisms and hydraulic properties of fault zones in unconsolidated
1010 sediments; the Roer Valley Rift System, The Netherlands.
1011 *Hydrogeology Journal*, 11(3): 319-332.
- 1012 Billi, A., Salvini, F. and Storti, F., 2003. The damage zone-fault core
1013 transition in carbonate rocks: implications for fault growth, structure
1014 and permeability. *Journal of Structural Geology*, 25(11): 1779-1794.
- 1015 Bjorkum, P.A., 1996. How important is pressure in causing dissolution of
1016 quartz in sandstones? *Journal of Sedimentary Research*, 66(1): 147-
1017 154.
- 1018 Blenkinsop, T.G., 1991. Cataclasis and processes of particle size reduction.
1019 *Pure and Applied Geophysics*, 136(1): 59-86.
- 1020 Borg, I., Friedman, M., Handin, J. and Higgs, D.V., 1960. Chapter 6:
1021 Experimental Deformation of St. Peter Sand: A Study of Cataclastic
1022 Flow. *Geological Society of America Memoirs*, 79: 133-192.
- 1023 Bouvier, J.D., Kaarssijpesteijn, C.H., Kluesner, D.F., Onyejekwe, C.C. and
1024 Vanderpal, R.C., 1989. Three-Dimensional Seismic Interpretation and
1025 Fault Sealing Investigations, Nun River Field, Nigeria. *American
1026 Association of Petroleum Geologists Bulletin*, 73(11): 1397-1414.

- 1027 Braathen, A., Tveranger, J., Fossen, H., Skar, T., Cardozo, N., Semshaug,
1028 S., Bastesen, E. and Sverdrup, E., 2009. Fault facies and its
1029 application to sandstone reservoirs. *AAPG bulletin*, 93(7): 891-917.
- 1030 Brogi, A. and Novellino, R., 2015. Low Angle Normal Fault (LANF)-zone
1031 architecture and permeability features in bedded carbonate from inner
1032 Northern Apennines (Rapolano Terme, Central Italy). *Tectonophysics*,
1033 638(0): 126-146.
- 1034 Caine, J.S., Evans, J.P. and Forster, C.B., 1996. Fault zone architecture and
1035 permeability structure. *Geology*, 24(11): 1025-1028.
- 1036 Cecil, C.B. and Heald, M.T., 1971. Experimental investigation of the effects
1037 of grain coatings on quartz growth. *Journal of Sedimentary Petrology*,
1038 41: 582-584.
- 1039 Cervený, K., Davies, R., Dudley, G., Fox, R., Kaufman, P., Knipe, R.J. and
1040 Krantz, B., 2004. Reducing Uncertainty with Fault-Seal Analysis.
1041 *Oilfield Review*, 16(4): 38-51.
- 1042 Childs, C., Manzocchi, T., Walsh, J.J., Bonson, C.G., Nicol, A. and Schöpfer,
1043 M.P.J., 2009. A geometric model of fault zone and fault rock thickness
1044 variations. *Journal of Structural Geology*, 31(2): 117-127.
- 1045 Childs, C., Nicol, A., Walsh, J.J. and Watterson, J., 1996a. Growth of
1046 vertically segmented normal faults. *Journal of Structural Geology*,
1047 18(12): 1389-1397.
- 1048 Childs, C., Watterson, J. and Walsh, J.J., 1996b. A model for the structure
1049 and development of fault zones. *Journal of the Geological Society*,
1050 153(3): 337-340.
- 1051 Choi, J.H., Yang, S.J., Han, S.R. and Kim, Y.S., 2015. Fault zone evolution
1052 during Cenozoic tectonic inversion in SE Korea. *Journal of Asian
1053 Earth Sciences*, 98: 167–177.
- 1054 Ciftci, N.B., Giger, S.B. and Clennell, M.B., 2013. Three-dimensional
1055 structure of experimentally produced clay smears: Implications for
1056 fault seal analysis. *American Association of Petroleum Geologists
1057 Bulletin*, 97(5): 733-757.
- 1058 Clarke, S.M., Burley, S.D. and Williams, G.D., 2005. A three-dimensional
1059 approach to fault seal analysis: fault-block juxtaposition & argillaceous
1060 smear modelling. *Basin Research*, 17(2): 269-288.
- 1061 Collettini, C., Carpenter, B.M., Viti, C., Cruciani, F., Mollo, S., Tesei, T.,
1062 Trippetta, F., Valoroso, L. and Chiaraluce, L., 2014. Fault structure
1063 and slip localization in carbonate-bearing normal faults: An example
1064 from the Northern Apennines of Italy. *Journal of Structural Geology*,
1065 67, Part A(0): 154-166.
- 1066 Cowie, P.A., Knipe, R.J. and Main, I.G., 1996. Introduction to the Special
1067 Issue: Scaling Laws for fault and fracture populations - analyses and
1068 applications. *Journal of Structural Geology*, 18(2-3): v-xi.
- 1069 Cowie, P.A. and Scholz, C.H., 1992. Displacement-length scaling
1070 relationship for faults: data synthesis and discussion. *Journal of
1071 Structural Geology*, 14(10): 1149-1156.
- 1072 Cowie, P.A., Vanneste, C. and Sornette, D., 1993. Statistical physics model
1073 for the spatiotemporal evolution of faults. *Journal of Geophysical
1074 Research*, 98(B12): 21809-21821.
- 1075 Crawford, B.R., 1998. Experimental fault sealing: shear band permeability
1076 dependency on cataclastic fault gouge characteristics. *Geological
1077 Society, London, Special Publications*, 127(1): 27-47.

1078 Davatzes, N. and Aydin, A., 2005. Distribution and nature of fault
1079 architecture in a layered sandstone and shale sequence: An example
1080 from the Moab fault, Utah. in R. Sorkhabi and Y. Tsuji, eds., Faults,
1081 fluid flow, and petroleum traps: American Association of Petroleum
1082 Geologists Memoir, 85: 153-180.

1083 Dewers, T. and Ortoleva, P., 1991. Influences of clay minerals on sandstone
1084 cementation and pressure solution. *Geology*, 19(10): 1045-1048.

1085 Dewers, T. and Ortoleva, P.J., 1990. Interaction of reaction, mass transport,
1086 and rock deformation during diagenesis: mathematical modelling of
1087 intergranular pressure solution, stylolites, and differential
1088 compaction/cementation. in I. D. Meshri and P. J. Ortoleva, eds.,
1089 Prediction of Reservoir Quality through Chemical Modelling: American
1090 Association of Petroleum Geologists Memoir, 49: 147-160.

1091 Egholm, D.L., Clausen, O.R., Sandiford, M., Kristensen, M.B. and Korstgård,
1092 J.A., 2008. The mechanics of clay smearing along faults. *Geology*,
1093 36(10): 787-790.

1094 Eisenstadt, G. and De Paor, D.G., 1987. Alternative model of thrust-fault
1095 propagation. *Geology*, 15(7): 630-633.

1096 Engelder, J.T., 1974. Cataclasis and the Generation of Fault Gouge.
1097 *Geological Society of America Bulletin*, 85(10): 1515-1522.

1098 Fachri, M., Rotevatn, A. and Tveranger, J., 2013a. Fluid flow in relay zones
1099 revisited: Towards an improved representation of small-scale
1100 structural heterogeneities in flow models. *Marine and Petroleum
1101 Geology*, 46(0): 144-164.

1102 Fachri, M., Tveranger, J., Braathen, A. and Schueller, S., 2013b. Sensitivity
1103 of fluid flow to deformation-band damage zone heterogeneities: A
1104 study using fault facies and truncated Gaussian simulation. *Journal of
1105 Structural Geology*, 52: 60-79.

1106 Fachri, M., Tveranger, J., Cardozo, N. and Pettersen, O., 2011. The impact
1107 of fault envelope structure on fluid flow: A screening study using fault
1108 facies. *AAPG bulletin*, 95(4): 619-648.

1109 Faulkner, D.R., Jackson, C.A.L., Lunn, R.J., Schlische, R.W., Shipton, Z.K.,
1110 Wibberley, C.A.J. and Withjack, M.O., 2010. A review of recent
1111 developments concerning the structure, mechanics and fluid flow
1112 properties of fault zones. *Journal of Structural Geology*, 32(11): 1557-
1113 1575.

1114 Faulkner, D.R., Lewis, A.C. and Rutter, E.H., 2003. On the internal structure
1115 and mechanics of large strike-slip fault zones: field observations of
1116 the Carboneras fault in southeastern Spain. *Tectonophysics*, 367(3):
1117 235–251.

1118 Fisher, Q.J., Casey, M., Harris, S.D. and Knipe, R.J., 2003. Fluid-flow
1119 properties of faults in sandstone: The importance of temperature
1120 history. *Geology*, 31(11): 965-968.

1121 Fisher, Q.J. and Jolley, S.J., 2007. Treatment of faults in production
1122 simulation models. Geological Society, London, Special Publications,
1123 292: 219-233.

1124 Fisher, Q.J. and Knipe, R.J., 1998. Fault sealing processes in siliciclastic
1125 sediments. Geological Society, London, Special Publications, 147:
1126 117-134.

1127 Fisher, Q.J. and Knipe, R.J., 2001. The permeability of faults within
1128 siliciclastic petroleum reservoirs of the North Sea and Norwegian

- 1129 Continental Shelf. *Marine and Petroleum Geology*, 18(10): 1063-
1130 1081.
- 1131 Fisher, Q.J., Knipe, R.J. and Worden, R.H., 2009. Microstructures of
1132 Deformed and Non-Deformed Sandstones from the North Sea:
1133 Implications for the Origins of Quartz Cement in Sandstones. in R. H.
1134 Worden and S. Morad, eds., *Quartz Cementation in Sandstones*,
1135 Blackwell Publishing Ltd., Oxford, UK, 14: 129-146.
- 1136 Fondriest, M., Smith, S.A.F., Toro, G.D., Zampieri, D. and Mitterpergher, S.,
1137 2012. Fault zone structure and seismic slip localization in dolostones,
1138 an example from the Southern Alps, Italy. *Journal of Structural*
1139 *Geology*, 45: 52–67.
- 1140 Fossen, H. and Bale, A., 2007. Deformation bands and their influence on
1141 fluid flow. *Aapg Bulletin*, 91(12): 1685-1700.
- 1142 Fossen, H., Schultz, R.A., Shipton, Z.K. and Mair, K., 2007. Deformation
1143 bands in sandstone: a review. *Journal of the Geological Society*,
1144 164(4): 755-769.
- 1145 Fossen, H., Schultz, R.A. and Torabi, A., 2011. Conditions and implications
1146 for compaction band formation in the Navajo Sandstone, Utah.
1147 *Journal of Structural Geology*, 33(10): 1477-1490.
- 1148 Fulljames, J.R., Zijerveld, L.J.J. and Franssen, R.C.M.W., 1997. Fault seal
1149 processes: systematic analysis of fault seals over geological and
1150 production time scales. In: P. Møller-Pedersen and A.G. Koestler
1151 (Editors), *Norwegian Petroleum Society Special Publications*, pp. 51-
1152 59.
- 1153 Gibson, R.G., 1994. Fault-Zone Seals in Siliciclastic Strata of the Columbus
1154 Basin, Offshore Trinidad. *American Association of Petroleum*
1155 *Geologists Bulletin*, 78(9): 1372-1385.
- 1156 Handin, J., Hager Jr, R.V., Friedman, M. and Feather, J.N., 1963.
1157 Experimental deformation of sedimentary rocks under confining
1158 pressure: pore pressure tests. *American Association of Petroleum*
1159 *Geologists Bulletin*, 47(5): 717-755.
- 1160 Harris, S.D., Vaszi, A.Z. and Knipe, R.J., 2007. Three-dimensional upscaling
1161 of fault damage zones for reservoir simulation. *Geological Society*,
1162 London, Special Publications, 292: 353-374.
- 1163 Heald, M.T., 1955. Stylolites in Sandstones. *The Journal of Geology*, 63(2):
1164 101-114.
- 1165 Heynekamp, M.R., Goodwin, L.B., Mozley, P.S. and Haneberg, W.C., 1999.
1166 Controls on fault-zone architecture in poorly lithified sediments, Rio
1167 Grande Rift, New Mexico: Implications for fault-zone permeability and
1168 fluid flow, *Faults and Subsurface Fluid Flow in the Shallow Crust*.
1169 Washington, DC, AGU. *Geophys. Monogr. Ser.*, pp. 27-49.
- 1170 Hill, K.C., Keetley, J.T., Kendrick, R.D. and Sutriyono, E., 2004. Structure
1171 and hydrocarbon potential of the New Guinea Fold Belt. in K. R.
1172 McClay, eds., *Thrust tectonics and hydrocarbon systems*: American
1173 Association of Petroleum Geologists *Memoir*, 82: 494-514.
- 1174 Indrevær, K., Stunitz, H. and Bergh, S.G., 2014. On Palaeozoic–Mesozoic
1175 brittle normal faults along the SW Barents Sea margin: fault
1176 processes and implications for basement permeability and margin
1177 evolution. *Journal of the Geological Society*, 171(6): 831-846.
- 1178 Ingram, G.M., Chisholm, T.J., Grant, C.J., Hedlund, C.A., Stuart-Smith, P.
1179 and Teasdale, J., 2004. Deepwater North West Borneo: hydrocarbon

1180 accumulation in an active fold and thrust belt. *Marine and Petroleum*
1181 *Geology*, 21(7): 879-887.

1182 Jolley, S.J., Barr, D., Walsh, J.J. and Knipe, R.J., 2007a. Structurally
1183 complex reservoirs: an introduction. Geological Society, London,
1184 Special Publications, 292: 1-24.

1185 Jolley, S.J., Dijk, H., Lamens, J.H., Fisher, Q.J., Manzocchi, T., Eikmans, H.
1186 and Huang, Y., 2007b. Faulting and fault sealing in production
1187 simulation models: Brent Province, northern North Sea. *Petroleum*
1188 *Geoscience*, 13(4): 321-340.

1189 Jones, R.M. and Hillis, R.R., 2003. An integrated, quantitative approach to
1190 assessing fault-seal risk. *AAPG bulletin*, 87(3): 507-524.

1191 Knipe, R.J., 1989. Deformation Mechanisms - Recognition from Natural
1192 Tectonites. *Journal of Structural Geology*, 11(1-2): 127-146.

1193 Knipe, R.J., 1992a. Faulting processes and fault seal. In: R.M. Larsen, H.
1194 Brekke, B.T. Larsen and E. Talleraas (Editors), *Norwegian Petroleum*
1195 *Society Special Publications*, pp. 325-342.

1196 Knipe, R.J., 1992b. Faulting processes, seal evolution, and reservoir
1197 discontinuities: An integrated analysis of the ULA Field, Central
1198 Graben, North Sea, Abstracts of the Petroleum Group meeting on
1199 collaborative research programme in petroleum geoscience between
1200 UK Higher Education Institutes and the Petroleum Industry,
1201 Geological Society, London.

1202 Knipe, R.J., 1993a. The Influence of Fault Zone Processes and Diagenesis
1203 on Fluid Flow. *Diagenesis and Basin Development*(36): 135-154.

1204 Knipe, R.J., 1993b. Micromechanisms of deformation and fluid flow
1205 behaviour during faulting. The mechanical behavior of fluids in fault
1206 zones: USGS Open-File Report: 94-228.

1207 Knipe, R.J., 1994. Fault zone geometry and behaviour: the importance of
1208 damage zone evolution. Abstracts of Meetings Modern Developments
1209 in Structural Interpretation, Geological Society, London.

1210 Knipe, R.J., 1997. Juxtaposition and seal diagrams to help analyze fault
1211 seals in hydrocarbon reservoirs. *American Association of Petroleum*
1212 *Geologists Bulletin*, 81(2): 187-195.

1213 Knipe, R.J., Fisher, R.J., Jones, G., Clennell, M.R., Farmer, A.B., Harrison,
1214 a., Kidd, B., McAllister, E., R., P.J. and White, E.A., 1997. Fault seal
1215 analysis: successful methodologies, application and future directions.
1216 *Norwegian Petroleum Society Special Publications*, 7: 15-40.

1217 Knipe, R.J., Jones, G. and Fisher, Q.J., 1998. Faulting, fault sealing and fluid
1218 flow in hydrocarbon reservoirs: an introduction. Geological Society,
1219 London, Special Publications, 147(1): vii-xxi.

1220 Knott, S.D., 1993. Fault Seal Analysis in the North-Sea. *American*
1221 *Association of Petroleum Geologists Bulletin*, 77(5): 778-792.

1222 Kolyukhin, D., Schueller, S., Espedal, M. and Fossen, H., 2010. Deformation
1223 band populations in fault damage zone—impact on fluid flow.
1224 *Computational Geosciences*, 14(2): 231-248.

1225 Korneva, I., Tondi, E., Agosta, F., Rustichelli, A., Spina, V., Bitonte, R. and
1226 Di Cuia, R., 2014. Structural properties of fractured and faulted
1227 Cretaceous platform carbonates, Murge Plateau (southern Italy).
1228 *Marine and Petroleum Geology*, 57: 312-326.

1229 Lewis, G., Knipe, R.J. and Li, A., 2002. Fault seal analysis in unconsolidated
1230 sediments: a field study from kentucky, USA. In: G.K. Andreas and H.

- 1231 Robert (Editors), Norwegian Petroleum Society Special Publications,
1232 pp. 243-253.
- 1233 Lindsay, N.G., Murphy, F.C., Walsh, J.J. and Watterson, J., 1993. Outcrop
1234 Studies of Shale Smears on Fault Surface, The Geological Modelling
1235 of Hydrocarbon Reservoirs and Outcrop Analogues. Blackwell
1236 Publishing Ltd., pp. 113-123.
- 1237 Loveless, S., Bense, V. and Turner, J., 2011. Fault architecture and
1238 deformation processes within poorly lithified rift sediments, Central
1239 Greece. *Journal of Structural Geology*, 33(11): 1554-1568.
- 1240 Manzocchi, T., Childs, C. and Walsh, J.J., 2010. Faults and fault properties
1241 in hydrocarbon flow models. *Geofluids*, 10(1-2): 94-113.
- 1242 Manzocchi, T., Heath, A.E., Walsh, J.J. and Childs, C., 2002. The
1243 representation of two phase fault-rock properties in flow simulation
1244 models. *Petroleum Geoscience*, 8(2): 119-132.
- 1245 Manzocchi, T., Walsh, J.J., Nell, P. and Yielding, G., 1999. Fault
1246 transmissibility multipliers for flow simulation models. *Petroleum
1247 Geoscience*, 5(1): 53-63.
- 1248 McGrath, A.G. and Davison, I., 1995. Damage zone geometry around fault
1249 tips. *Journal of Structural Geology*, 17(7): 1011-1024.
- 1250 Odling, N.E., Harris, S.D. and Knipe, R., 2004. Permeability scaling
1251 properties of fault damage zones in siliclastic rocks. *Journal of
1252 Structural Geology*, 26(9): 1727-1747.
- 1253 Oelkers, E.H., Bjorkum, P.A. and Murphy, W.M., 1996. A petrographic and
1254 computational investigation of quartz cementation and porosity
1255 reduction in North Sea sandstones. *American Journal of Science*,
1256 296(4): 420-452.
- 1257 Ottesen Ellevset, S., Knipe, R.J., Svava Olsen, T., Fisher, Q.J. and Jones,
1258 G., 1998. Fault controlled communication in the Sleipner Vest Field,
1259 Norwegian Continental Shelf; detailed, quantitative input for reservoir
1260 simulation and well planning. Geological Society, London, Special
1261 Publications, 147(1): 283-297.
- 1262 Pang, X.Q., Li, Y.X. and Jiang, Z.X., 2004. Key geological controls on
1263 migration and accumulation for hydrocarbons derived from mature
1264 source rocks in Qaidam Basin. *Journal of Petroleum Science and
1265 Engineering*, 41(1-3): 79-95.
- 1266 Peacock, D.C.P. and Sanderson, D.J., 1991. Displacements, segment
1267 linkage and relay ramps in normal fault zones. *Journal of Structural
1268 Geology*, 13(6): 721-733.
- 1269 Peacock, D.C.P. and Sanderson, D.J., 1992. Effects of layering and
1270 anisotropy on fault geometry. *Journal of the Geological Society*,
1271 149(5): 793-802.
- 1272 Peacock, D.C.P. and Sanderson, D.J., 1994. Geometry and development of
1273 relay ramps in normal fault systems. *American Association of
1274 Petroleum Geologists Bulletin*, 78(2): 147-165.
- 1275 Pei, Y.W., 2013. Thrust fault evolution and hydrocarbon sealing behaviour,
1276 Qaidam basin, China. PhD Thesis, University of Leeds.
- 1277 Qu, D., Røe, P. and Tveranger, J., 2015. A method for generating volumetric
1278 fault zone grids for pillar gridded reservoir models. *Computers &
1279 Geosciences*, 81: 28-37.

- 1280 Rawling, G.C. and Goodwin, L.B., 2003. Cataclasis and particulate flow in
 1281 faulted, poorly lithified sediments. *Journal of Structural Geology*,
 1282 25(3): 317-331.
- 1283 Rawling, G.C. and Goodwin, L.B., 2006. Structural record of the mechanical
 1284 evolution of mixed zones in faulted poorly lithified sediments, Rio
 1285 Grande rift, New Mexico, USA. *Journal of Structural Geology*, 28(9):
 1286 1623-1639.
- 1287 Rawling, G.C., Goodwin, L.B. and Wilson, J.L., 2001. Internal architecture,
 1288 permeability structure, and hydrologic significance of contrasting fault-
 1289 zone types. *Geology*, 29(1): 43-46.
- 1290 Roche, V., Homberg, C. and Rocher, M., 2012. Architecture and growth of
 1291 normal fault zones in multilayer systems: A 3D field analysis in the
 1292 South-Eastern Basin, France. *Journal of Structural Geology*, 37(0):
 1293 19-35.
- 1294 Rotevatn, A. and Bastesen, E., 2014. Fault linkage and damage zone
 1295 architecture in tight carbonate rocks in the Suez Rift (Egypt):
 1296 implications for permeability structure along segmented normal faults.
 1297 *Geological Society, London, Special Publications*, 374(1): 79-95.
- 1298 Rotevatn, A., Fossen, H., Hesthammer, J., Aas, T.E. and Howell, J.A., 2007.
 1299 Are relay ramps conduits for fluid flow? Structural analysis of a relay
 1300 ramp in Arches National Park, Utah: in. *Geological Society of London*,
 1301 270(1).
- 1302 Rutter, E.H., 1983. Pressure solution in nature, theory and experiment.
 1303 *Journal of the Geological Society*, 140(5): 725-740.
- 1304 Schöpfer, M.P.J., Childs, C. and Walsh, J.J., 2006. Localisation of normal
 1305 faults in multilayer sequences. *Journal of Structural Geology*, 28(5):
 1306 816-833.
- 1307 Schowalter, T.T., 1979. Mechanics of secondary hydrocarbon migration and
 1308 entrapment. *American Association of Petroleum Geologists Bulletin*,
 1309 63(5): 723-760.
- 1310 Schultz, R.A. and Fossen, H., 2008. Terminology for structural
 1311 discontinuities. *Aapg Bulletin*, 92(7): 853-867.
- 1312 Scott, T.E. and Nielsen, K.C., 1991. The Effects of Porosity on the Brittle-
 1313 Ductile Transition in Sandstones. *Journal of Geophysical Research*,
 1314 96(B1): 405-414.
- 1315 Smith, D.A., 1966. Theoretical considerations of sealing and non-sealing
 1316 faults. *American Association of Petroleum Geologists Bulletin*, 50(2):
 1317 363-374.
- 1318 Smith, D.A., 1980. Sealing and nonsealing faults in Louisiana Gulf Coast salt
 1319 basin. *American Association of Petroleum Geologists Bulletin*, 64(2):
 1320 145-172.
- 1321 Spiers, C.J. and Schutjens, P.M.T.M., 1990. Densification of crystalline
 1322 aggregates by fluid-phase diffusional creep, *Deformation Processes*
 1323 *in Minerals, Ceramics and Rocks. The Mineralogical Society Series.*
 1324 *Springer Netherlands*, pp. 334-353.
- 1325 Tada, R. and Siever, R., 1989. Pressure Solution during Diagenesis. *Annual*
 1326 *Review of Earth and Planetary Sciences*, 17: 89-118.
- 1327 Torabi, A. and Berg, S.S., 2011. Scaling of fault attributes: A review. *Marine*
 1328 *and Petroleum Geology*, 28(8): 1444-1460.
- 1329 Tueckmantel, C., Fisher, Q.J., Knipe, R.J., Lickorish, H. and Khalil, S.M.,
 1330 2010. Fault seal prediction of seismic-scale normal faults in porous

1331 sandstone: A case study from the eastern Gulf of Suez rift, Egypt.
1332 Marine and Petroleum Geology, 27(2): 334-350.

1333 Tveranger, J., Skar, T. and Braathen, A., 2004. Incorporation of fault zones
1334 as volumes in reservoir models. Bolletino di Geofisica Teoretica et
1335 Applicata, 45: 316-318.

1336 Tveranger, J., Skauge, A., Braathen, A. and Skar, T., 2005. Centre for
1337 integrated petroleum research: Research activities with emphasis on
1338 fluid flow in fault zones. Norsk Geologisk Tidsskrift, 85(1-2): 63-71.

1339 Walderhaug, O., 1996. Kinetic modeling of quartz cementation and porosity
1340 loss in deeply buried sandstone reservoirs. American Association of
1341 Petroleum Geologists Bulletin, 80(5): 731-745.

1342 Walsh, J.J., Bailey, W.R., Childs, C., Nicol, A. and Bonson, C.G., 2003.
1343 Formation of segmented normal faults: a 3-D perspective. Journal of
1344 Structural Geology, 25(8): 1251-1262.

1345 Walsh, J.J., Watterson, J., Bailey, W.R. and Childs, C., 1999. Fault relays,
1346 bends and branch-lines. Journal of Structural Geology, 21(8-9):
1347 1019-1026.

1348 Walsh, J.J., Watterson, J., Heath, A.E. and Childs, C., 1998. Representation
1349 and scaling of faults in fluid flow models. Petroleum Geoscience, 4(3):
1350 241-251.

1351 Watts, N.L., 1987. Theoretical aspects of cap-rock and fault seals for single-
1352 and two-phase hydrocarbon columns. Marine and Petroleum
1353 Geology, 4(4): 274-307.

1354 Welch, M.J., Davies, R.K., Knipe, R.J. and Tueckmantel, C., 2009a. A
1355 dynamic model for fault nucleation and propagation in a mechanically
1356 layered section. Tectonophysics, 474(3-4): 473-492.

1357 Welch, M.J., Knipe, R.J., Souque, C. and Davies, R.K., 2009b. A Quadshear
1358 kinematic model for folding and clay smear development in fault
1359 zones. Tectonophysics, 471(3-4): 186-202.

1360 Welch, M.J., Souque, C., Davies, R.K. and Knipe, R.J., 2015. Using
1361 mechanical models to investigate the controls on fracture geometry
1362 and distribution in chalk. Geological Society, London, Special
1363 Publications, 406(1): 281-309.

1364 Yielding, G., Freeman, B. and Needham, D.T., 1997. Quantitative fault seal
1365 prediction. American Association of Petroleum Geologists Bulletin,
1366 81(6): 897-917.

1367 Yielding, G., Needham, T. and Jones, H., 1996. Sampling of fault
1368 populations using sub-surface data: a review. Journal of Structural
1369 Geology, 18(2): 135-146.

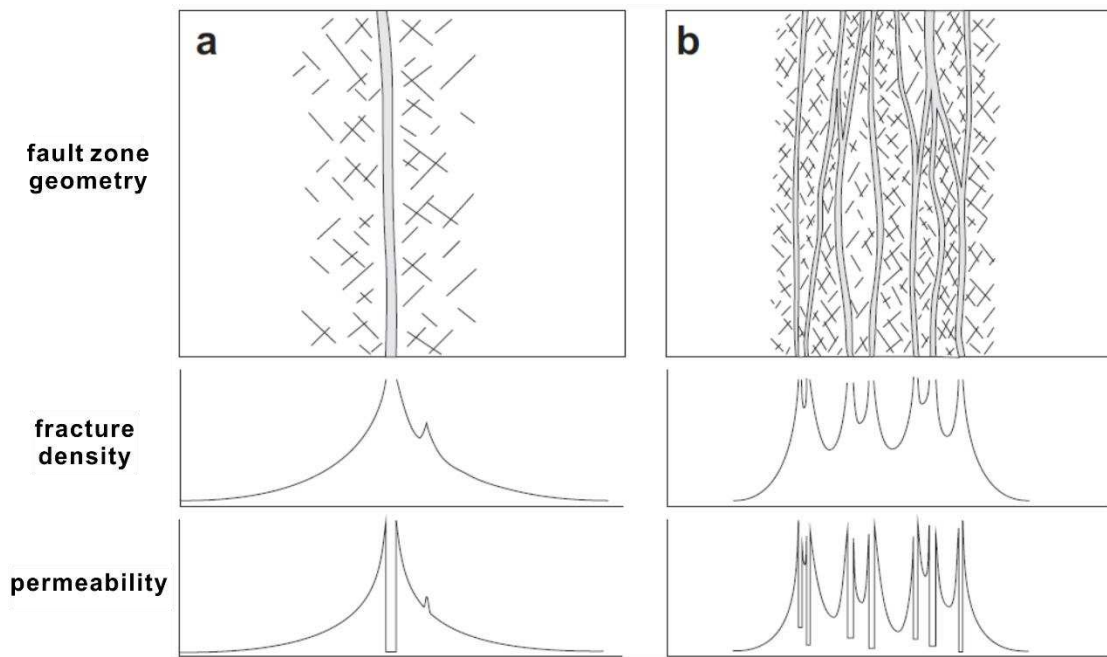
1370 Zhu, W.L. and Wong, T.F., 1997. The transition from brittle faulting to
1371 cataclastic flow: Permeability evolution. Journal of Geophysical
1372 Research, 102(B2): 3027-3041.

1373 Zijlstra, E.B., Reemst, P.H.M. and Fisher, Q.J., 2007. Incorporation of fault
1374 properties into production simulation models of Permian reservoirs
1375 from the southern North Sea. Geological Society, London, Special
1376 Publications, 292: 295-308.

1377

1378

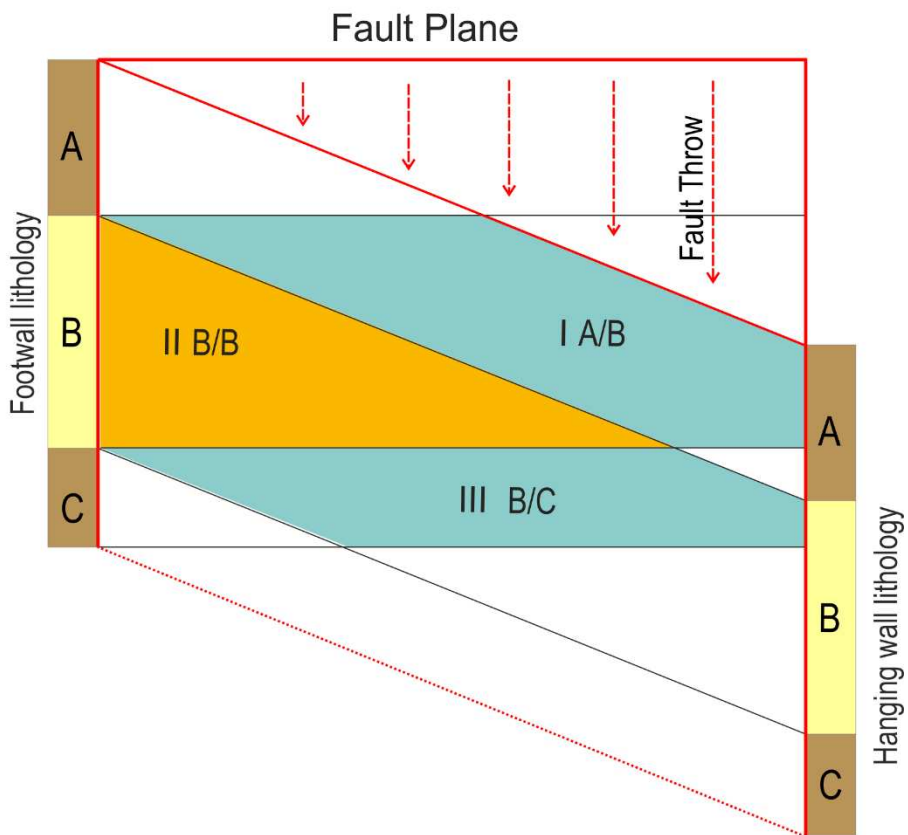
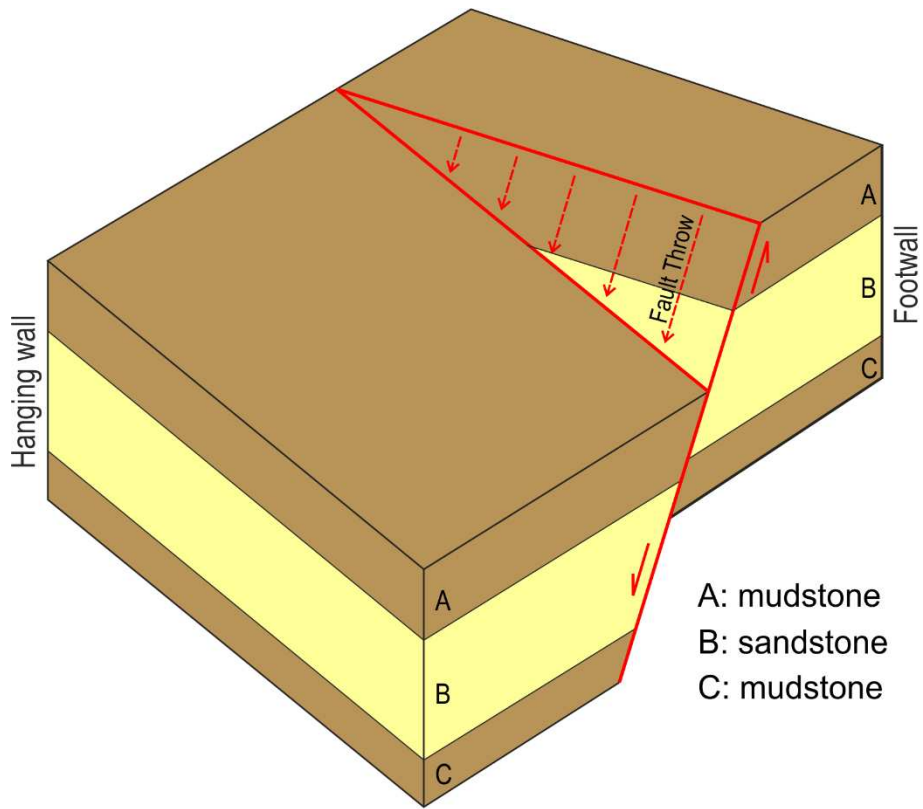
1379 **Figure 1**



1380

1381

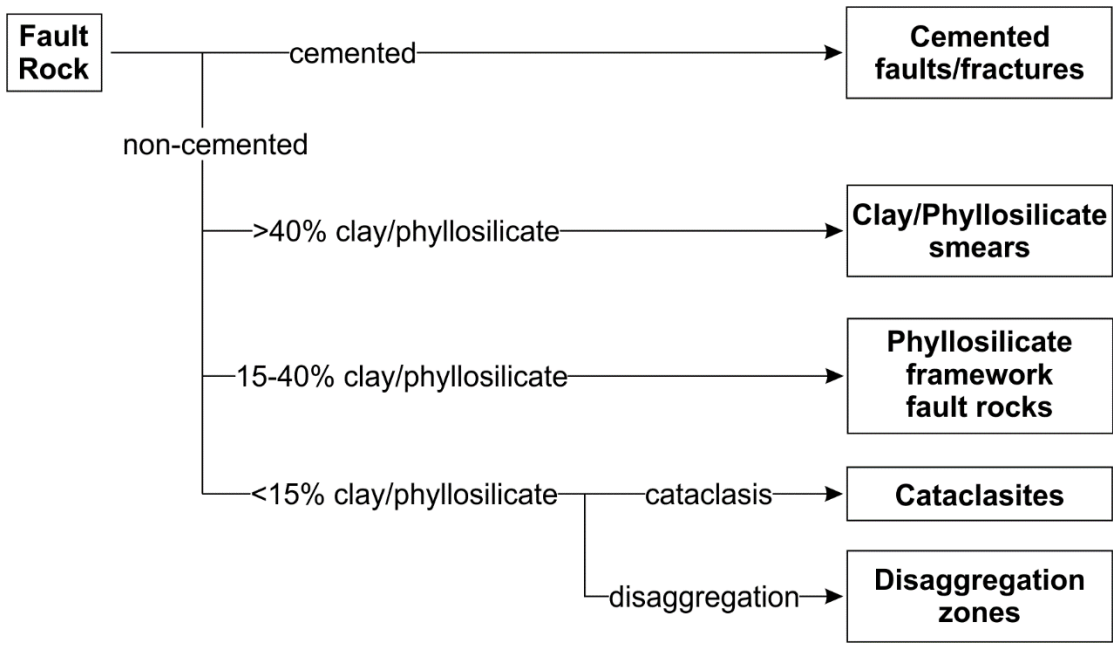
1382 **Figure 2**



1383

1384

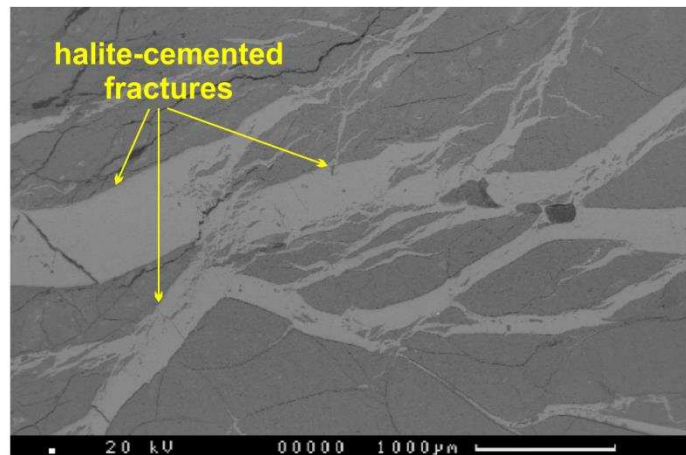
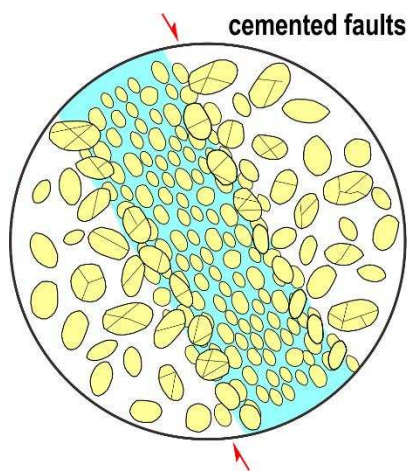
1385 **Figure 3**



1386

1387

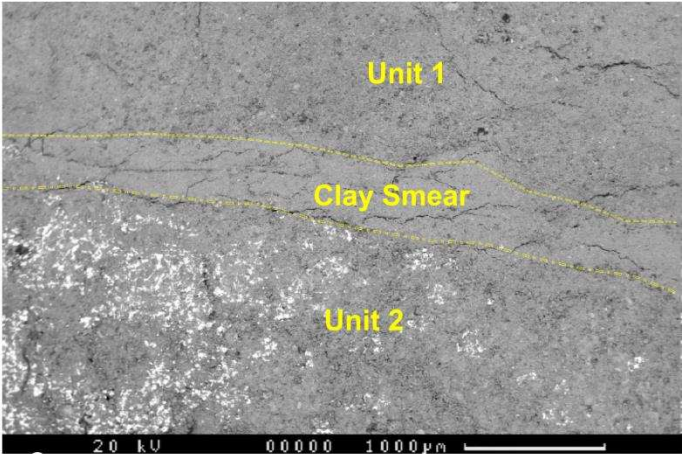
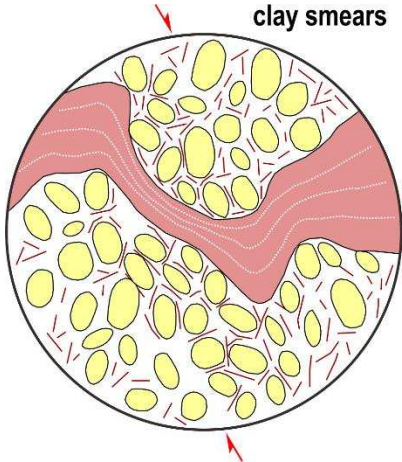
1388 **Figure 4**



1389

1390

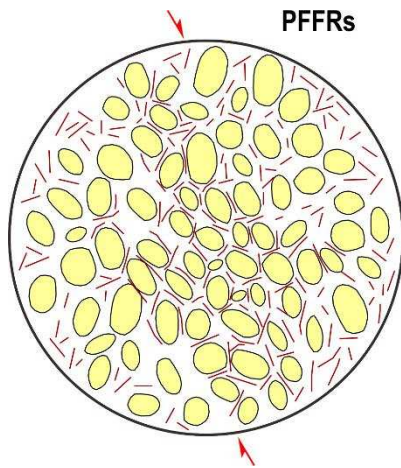
1391 **Figure 5**



1392

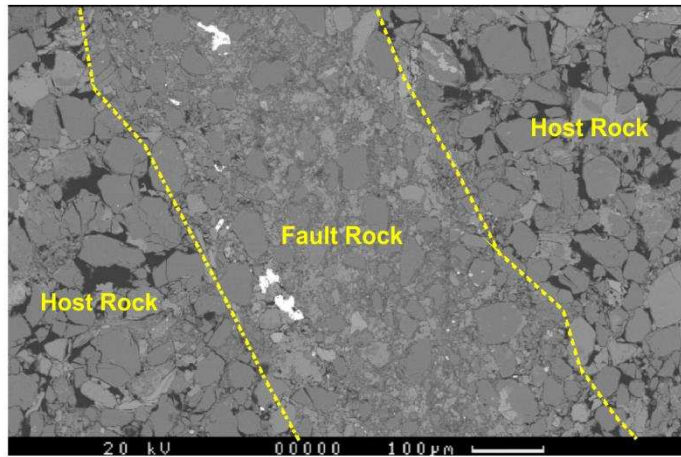
1393

1394 **Figure 6**

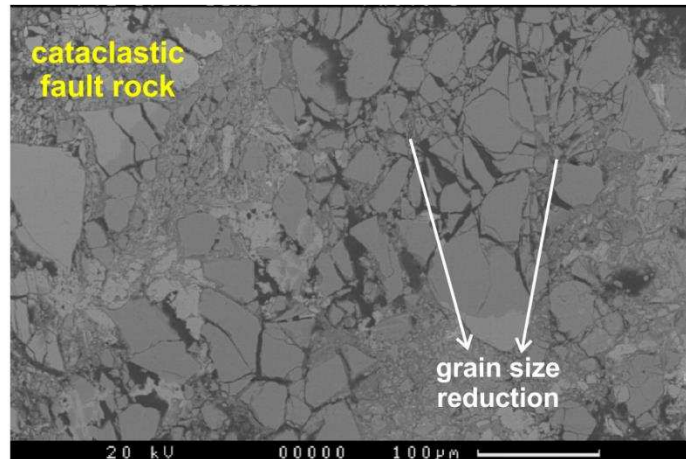
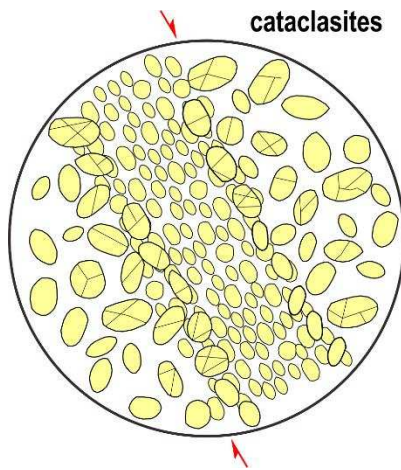


1395

1396



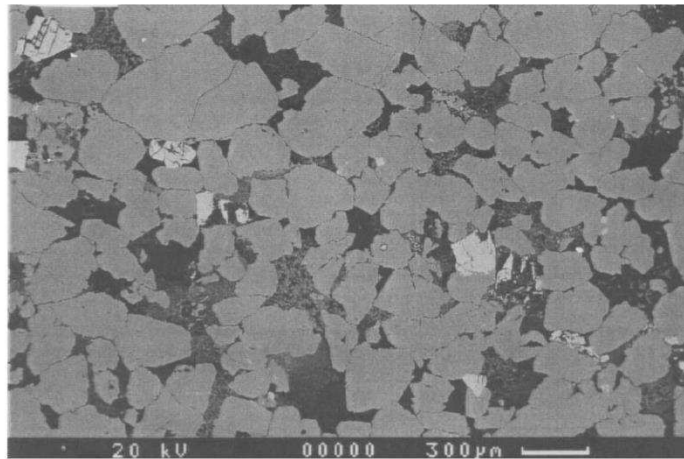
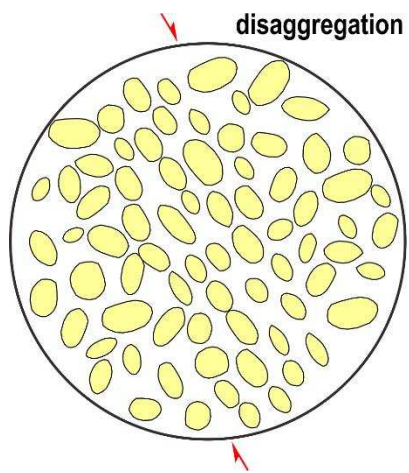
1397 **Figure 7**



1398

1399

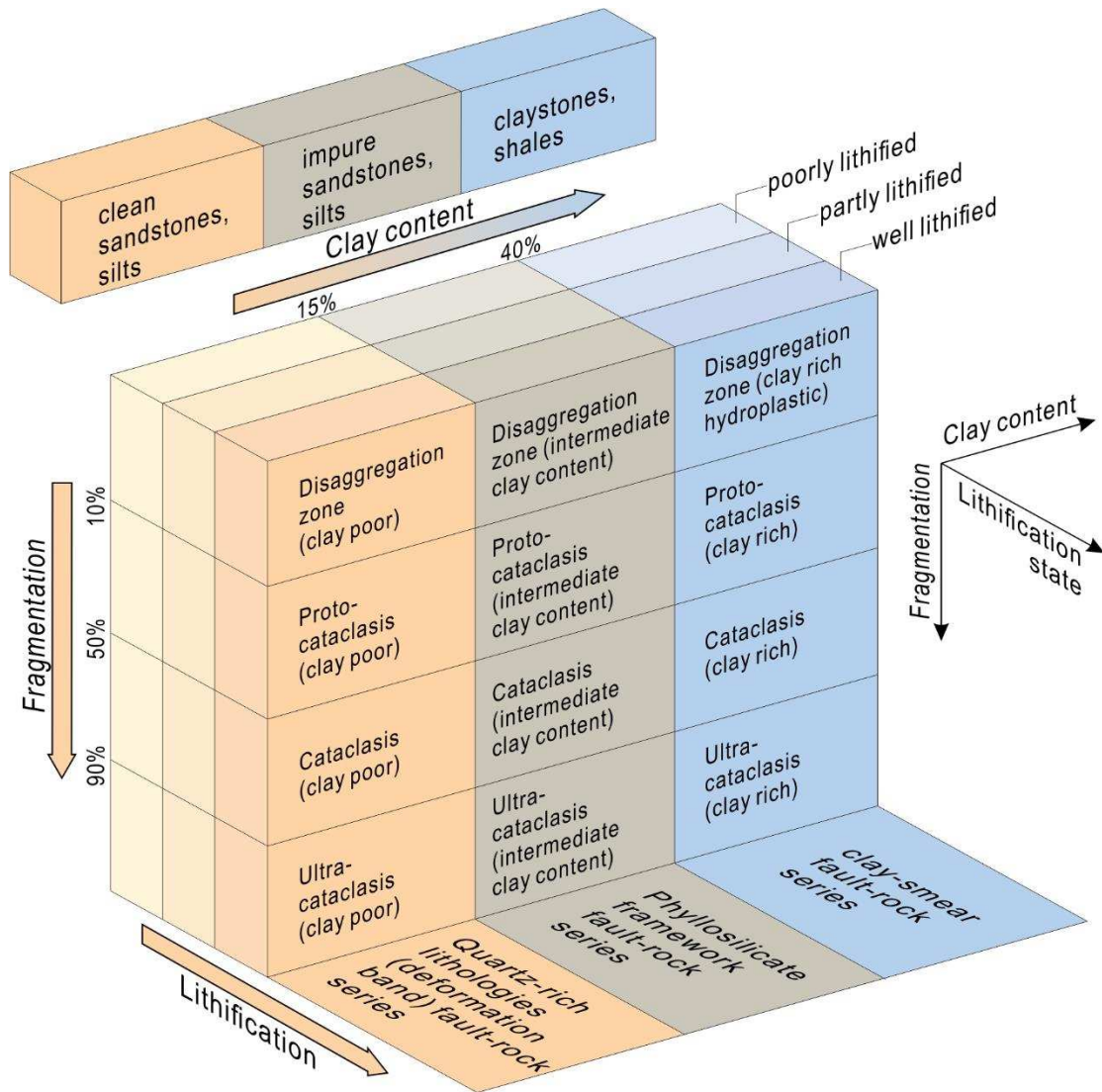
1400 **Figure 8**



1401

1402

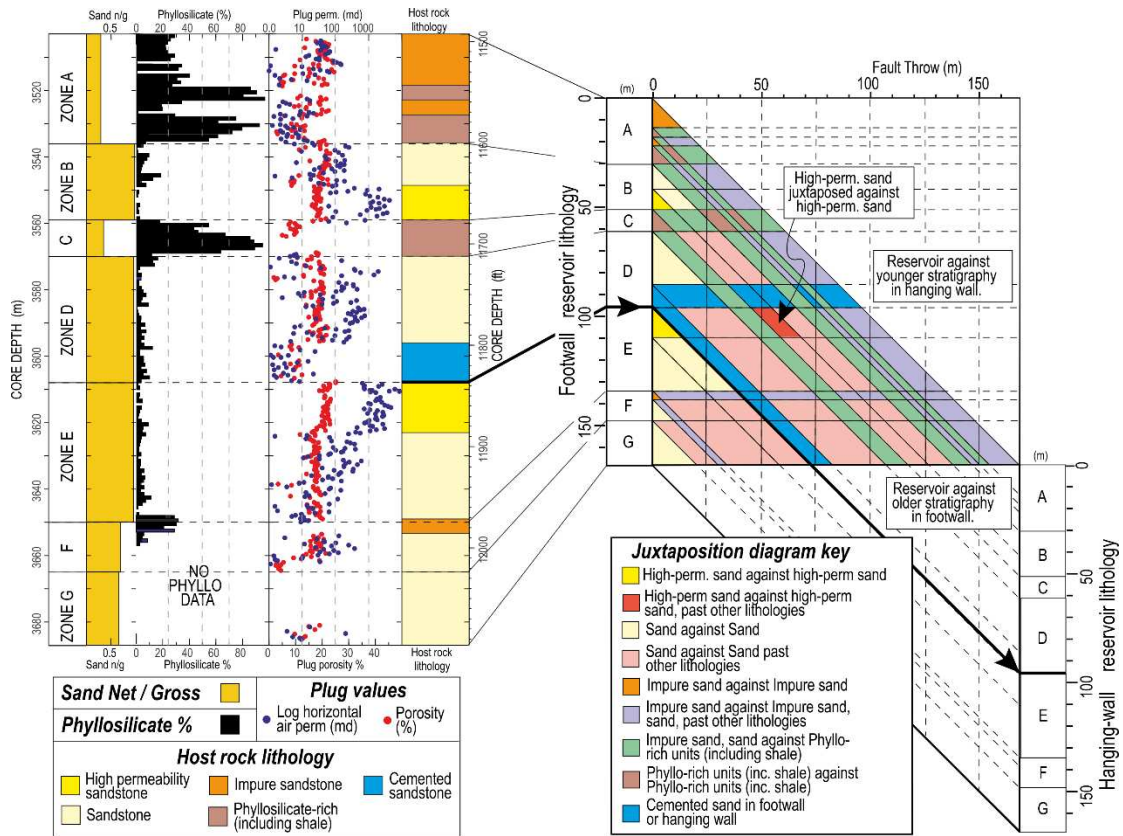
1403 **Figure 9**



1404

1405

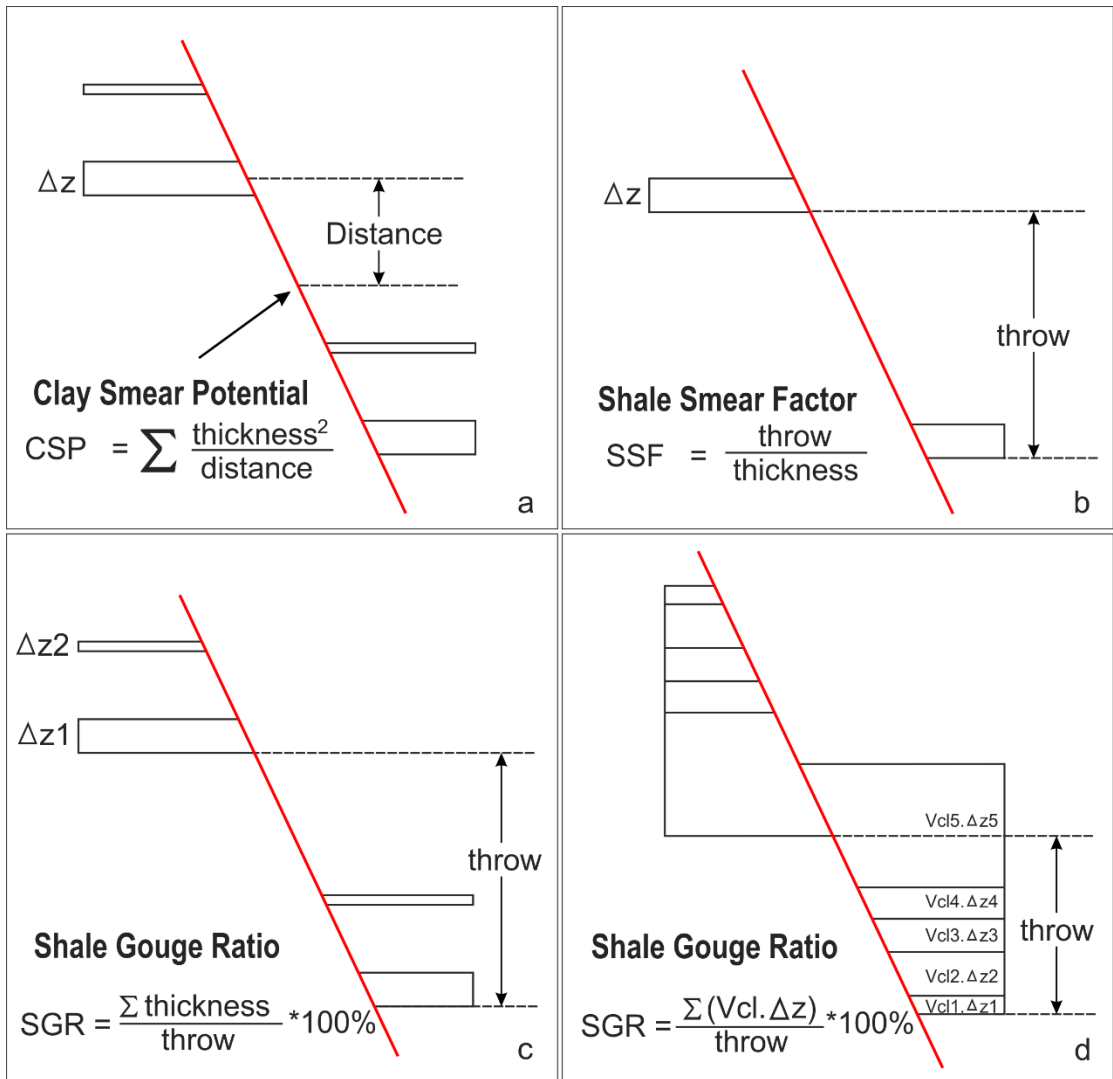
1406 **Figure 10**



1407

1408

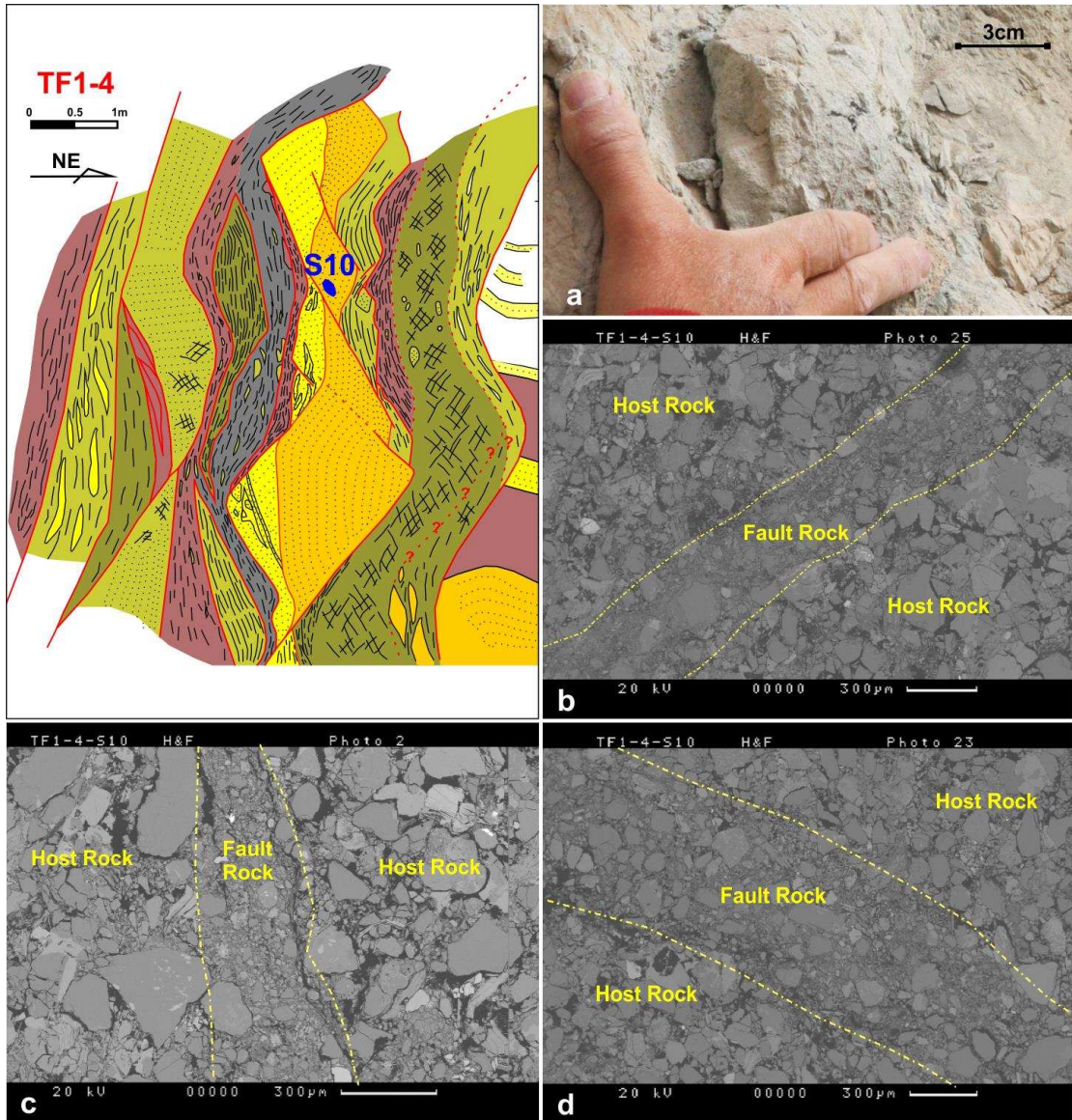
1409 **Figure 11**



1410

1411

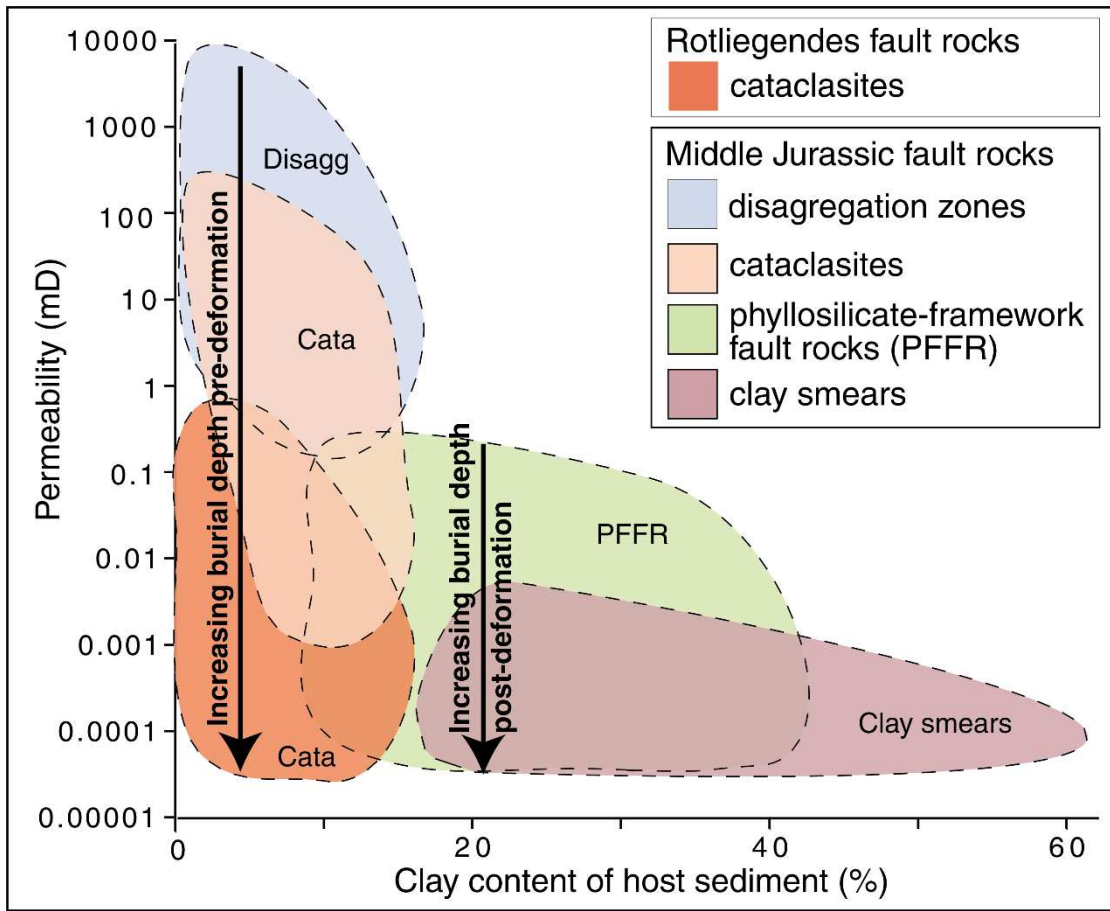
1412 **Figure 12**



1413

1414

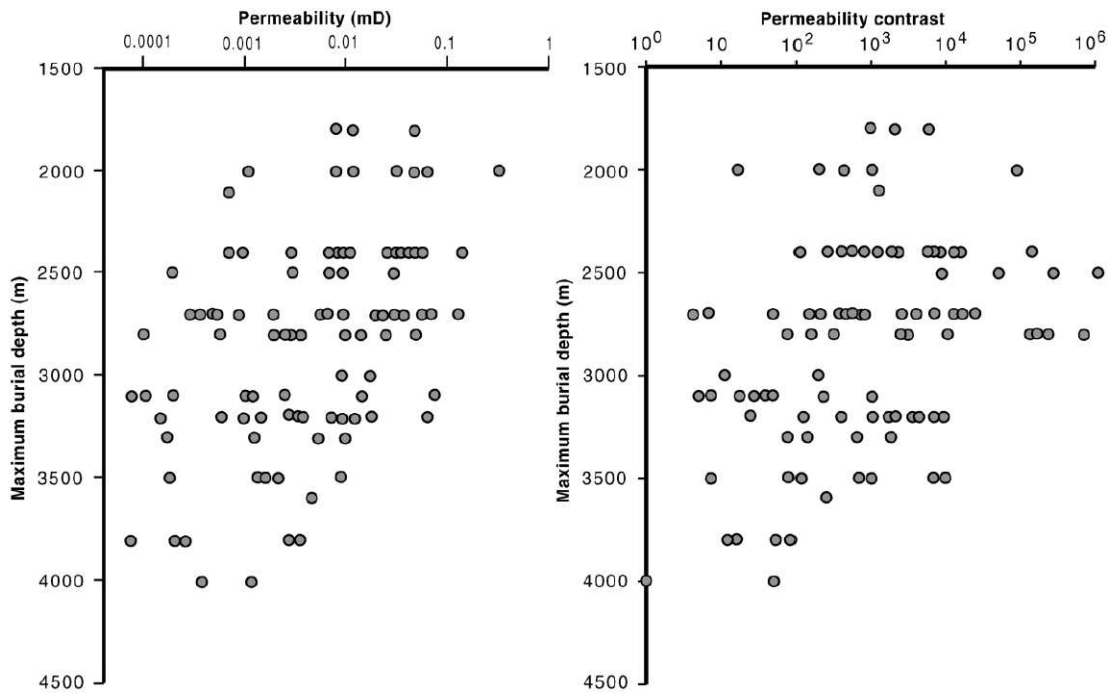
1415 **Figure 13**



1416

1417

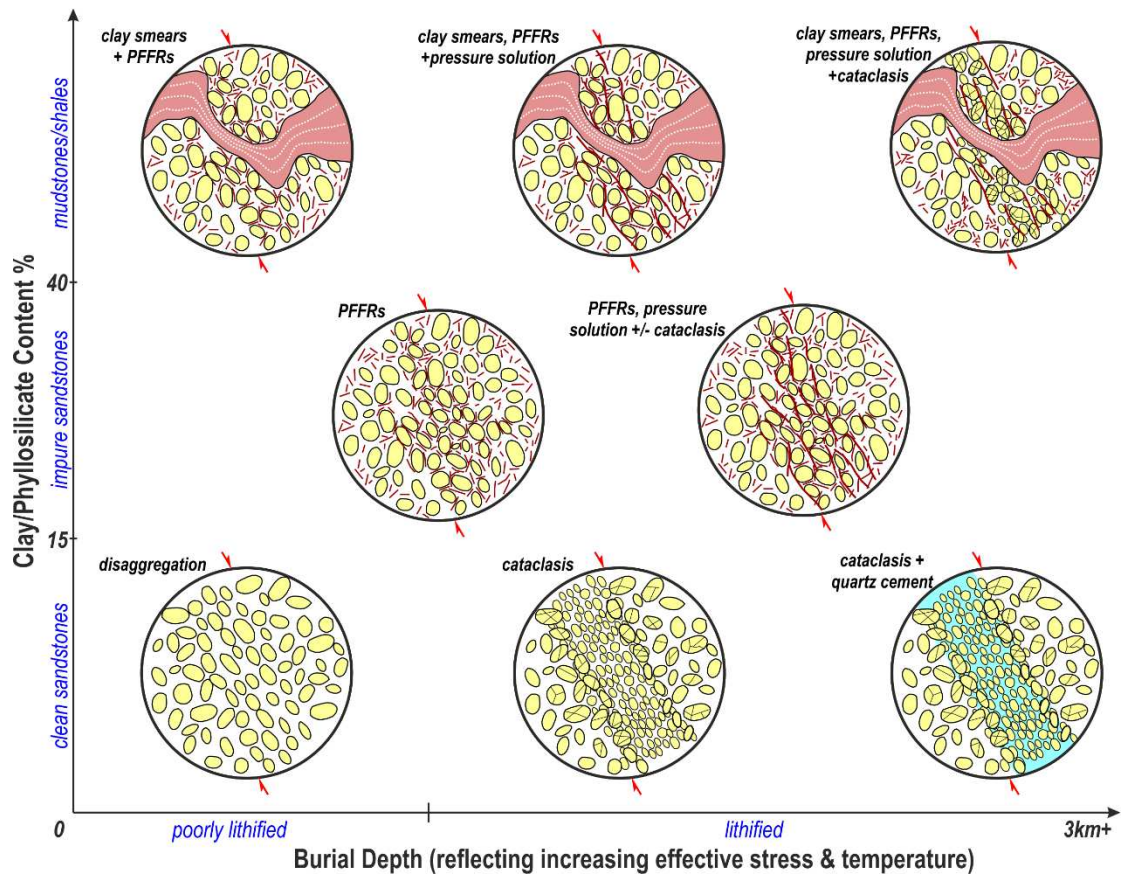
1418 **Figure 14**



1419

1420

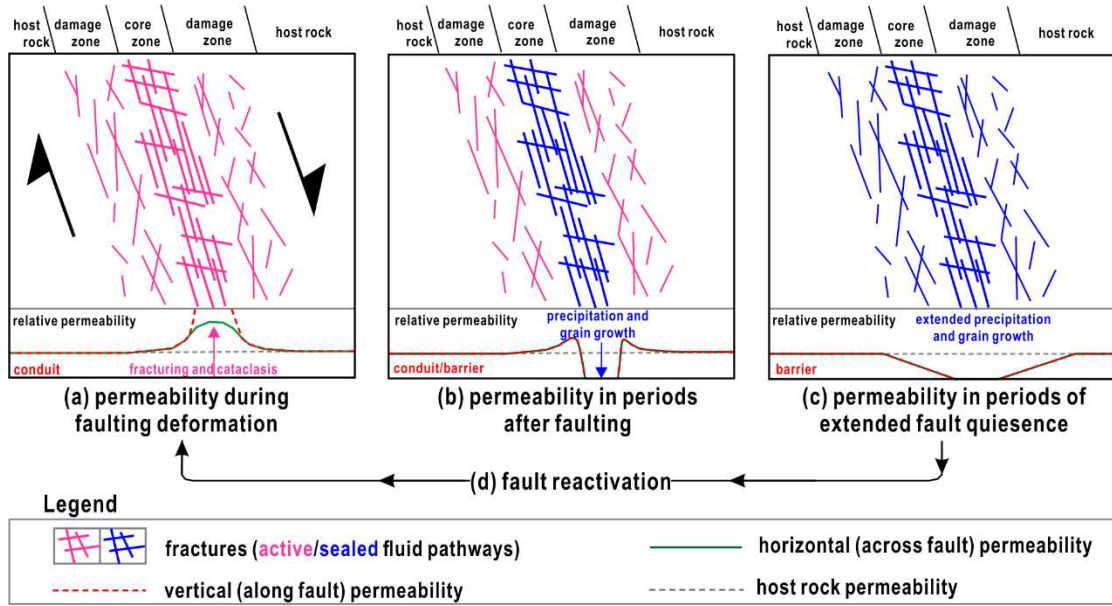
1421 **Figure 15**



1422

1423

1424 **Figure 16**



1425

1426

1427 **Table 1**

fault seal classifications	methods	references
	Allan map	Allan (1989)
	triangle juxtaposition diagram	Knipe (1997)
juxtaposition seals		Bouvier et. al., (1989)
	clay smear indices	Fulljames et al., (1997)
		Lindsay et al., (1993)
		Yielding et al., (1997)
		e.g., Knipe, (1992)
fault rock seals	micro-structural analysis	Fisher and Knipe, (1998)
		Ottesen Ellevset et al., (1998)
	petrophysical assessment	Fisher and Knipe (2001)
		Tueckmantel et. al., (2010)

1428

1429

1430